

PUBLIC ROADS

A JOURNAL OF HIGHWAY RESEARCH



UNITED STATES DEPARTMENT OF AGRICULTURE
BUREAU OF PUBLIC ROADS



VOL. 19, NO. 10



DECEMBER 1938



A SECTION OF U S 1 IN MAINE

PRINCIPLES OF SOIL MECHANICS INVOLVED IN THE DESIGN OF RETAINING WALLS AND BRIDGE ABUTMENTS

BY THE DIVISION OF TESTS, BUREAU OF PUBLIC ROADS

Reported by L. A. PALMER, Associate Chemist

IN A LARGE NUMBER of earth pressure and foundation problems the stresses found by the method based on elasticity are independent of elastic constants and are classified as problems of plane strain or plane deformation. These are problems involving two dimensions, and in their solution an analysis is made of the stresses in a vertical cross section of the earth embankment or supporting soil under a foundation. The limitations of the analytical method based on the assumption of the conditions of plane strain are indicated in this paper in the case of the supporting soil under abutments, piers, and retaining walls.

The principle of superimposition of different systems of loading is applied to problems of plane strain in deriving expressions for the greatest shearing stress in the undersoil below a symmetrical fill and a bridge abutment. The greatest unit shearing stress anywhere in the undersoil below a fill having equal side slopes and the top surface parallel to the subgrade surface is approximately $0.3p$, where p is the unit pressure of fill material at the subsoil level beneath the roadway. If $0.3p$ is less than the unit cohesion c of the undersoil, the latter is safe insofar as ultimate failure is concerned. However, when $0.3p$ exceeds c of the undersoil, it does not follow that failure is inevitable. In such a case Prandtl's formula is applied,

$$q = (c \cot \phi + wb' \cot \alpha) \left[\frac{1 + \sin \phi}{1 - \sin \phi} e^{\pi \tan \phi} - 1 \right]$$

where, with respect to the undersoil,

- q = supporting power,
- c = unit cohesion,
- w = unit weight,
- ϕ = angle of internal friction,
- $\alpha = 45^\circ - \phi/2$, and
- $b' = \frac{1}{2}$ the horizontal distance between the midpoints of the slopes of the symmetrical fill.

By this formula, the factor of safety against failure of the supporting soil is the ratio, $\frac{q}{p}$.

The maximum shearing stress in the soil below the base of an abutment subjected to a rotating moment producing a maximum vertical pressure p_0 at the toe is $\frac{p_0}{\pi}$. If $\frac{p_0}{\pi}$ is less than the cohesion of the undersoil, it will not fail under this stress. However, if $\frac{p_0}{\pi}$ exceeds c , it is necessary to determine the factor of safety $\frac{q}{p_0}$.

The object of this paper and that of a former one¹ is to make available for practicing engineers the method based on elasticity as a theoretical and practical approach to the study of earth problems. This method is particularly applicable to a large number of problems falling under the heading of plane strain. In this case the stresses found by the method based on elasticity are independent of the elastic constants, and the difference in the behavior of two different earth materials under loads which are equal and identical in distribution and with the same plane strain conditions is entirely a matter of difference in the relative displacements of the two stressed materials.

¹The Theory of Soil Consolidation and Testing of Foundation Soils, by L. A. Palmer and E. S. Barber, PUBLIC ROADS, vol. 18, No. 1, March 1937.

against failure, obtaining q from the formula,

$$q = \frac{2c}{\tan \alpha \sin^2 \alpha} + \frac{wa}{2 \tan \alpha} \left[\frac{1}{\tan^4 \alpha} - 1 \right] + \frac{wd}{\tan^4 \alpha}$$

where

- q = supporting power,
- c = unit cohesion,
- w = unit weight,
- $\alpha = 45^\circ - \phi/2$,
- d = depth of surcharge, and
- a = width of the base of the abutment.

The active and passive earth pressures and the earth pressure at rest, in the earth back of retaining walls, are easily determined by using the analytical method of Coulomb and the graphical method of Mohr. The conditions of plane strain are assumed in the application of both methods. Assuming a level earth surface back of the retaining wall, the expressions for the three earth pressures are

$$p_h \text{ (active)} = p_v \tan^2 (45^\circ - \phi/2) - 2c \tan (45^\circ - \phi/2)$$

$$p_h \text{ (at rest)} = K p_v$$

and

$$p_h \text{ (passive)} = p_v \tan^2 (45^\circ + \phi/2) + 2c \tan (45^\circ + \phi/2)$$

where

- ϕ = angle of internal friction of embankment material,
- c = unit cohesion of embankment material,
- K = coefficient of earth pressure at rest, of the embankment material,
- p_h = horizontal pressure, and
- p_v = vertical pressure.

The values, c , ϕ , and K are determined experimentally; p_h (active) is the smallest in magnitude of the earth pressures; p_h (passive) is the largest; and the earth pressure at rest, p_h (at rest) is intermediate in value between these two extremes. If the earth back of the wall moves outward when the wall fails by rotation about the base, the pressure is active. If movement of the wall is exceedingly small or zero, the pressure against it is earth pressure at rest. If the soil back of the wall is cohesive and of a nature such that it tends to expand or swell on wetting and to contract on drying, then, on swelling, the pressure exerted on the wall is passive earth pressure, and the wall should be designed to withstand passive earth pressure.

If the earth back of the wall is cohesionless material such as sand, the maximum pressure against the wall is earth pressure at rest. The value of K for sand has been reported as being within the limits 0.40 to 0.45.

The body under stress is assumed to be very long in comparison with its width, the length being in the Y direction. In this class of problems the stresses and strains are independent of one of the three rectangular coordinates, the Y coordinate in this paper. Examples of this class most frequently considered in textbooks are stresses in thick-walled tubes under internal pressure and stresses produced in a sheet of metal during rolling in which the dimension perpendicular to the direction of rolling is very large. Obviously, neither the tube nor the sheet are of "infinite length," an expression often used in purely mathematical treatments of such problems. In foundation problems, a foundation wall, a fill, an earth dam, a long retaining wall, or a bridge abutment with wing walls may be considered as examples of the plane strain problem.

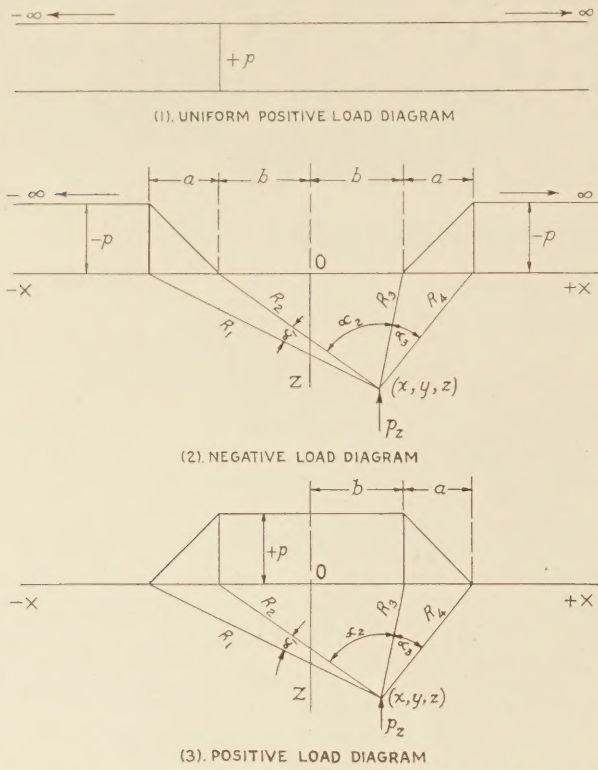


FIGURE 1.—A UNIFORM LOAD (1), SUPERIMPOSED ON A NEGATIVE LOAD DIAGRAM FOR A CUT (2), YIELDS THE POSITIVE LOAD DIAGRAM FOR A FILL (3).

CALCULATIONS INVOLVE SUPERIMPOSITION OF VARIOUS SYSTEMS OF LOADING

In this paper formulas will be derived for stresses in the supporting earth below (a) a symmetrical fill and (b) a bridge abutment subjected to a rotating moment of such a nature that a trapezoidal load distribution is transmitted by the abutment. Recourse will be had to well known methods of the superimposition of loading systems in these derivations. Further application of the principles of plane strain will be made in the analysis of the three types of earth pressures against retaining walls: (1) Earth pressure at rest; (2) active earth pressure; and (3) passive earth pressure. The method based on plastic equilibrium will be used in deriving an expression for the bearing capacity of soil supporting a bridge abutment and finally, there will be indicated by direct computations the extent of application of the methods based on plane strain in determining earth stresses below loaded rectangular areas of different sizes. These are topics of vital interest to bridge engineers and a continuation of the analysis much beyond the scope of this paper is needed.

Working formulas have been developed by S. D. Carothers² for several different systems of loading, all of which pertain to foundation problems of the plane strain class. It is possible to derive formulas for various additional loading systems by superimposing two or more of those already considered by Carothers. Two examples of this procedure will be given:

1. A uniform load, p , is superimposed on the negative load diagram for a cut so as to yield the load diagram for a fill (see

¹ Direct Determination of Stresses, by S. D. Carothers, Proceedings of the Royal Society of London, Series A, vol. 97, p. 110 et seq.

² Elastic Equivalence of Statically Equivalent Loads, by S. D. Carothers, Proceedings of the International Mathematical Congress, vol. 2, Toronto University Press, 1924, p. 527 et seq.

Test Loads on Foundations as Affected by Scale of Tested Area, by S. D. Carothers, Engineering, London, July 4, 1924, p. 1 et seq.

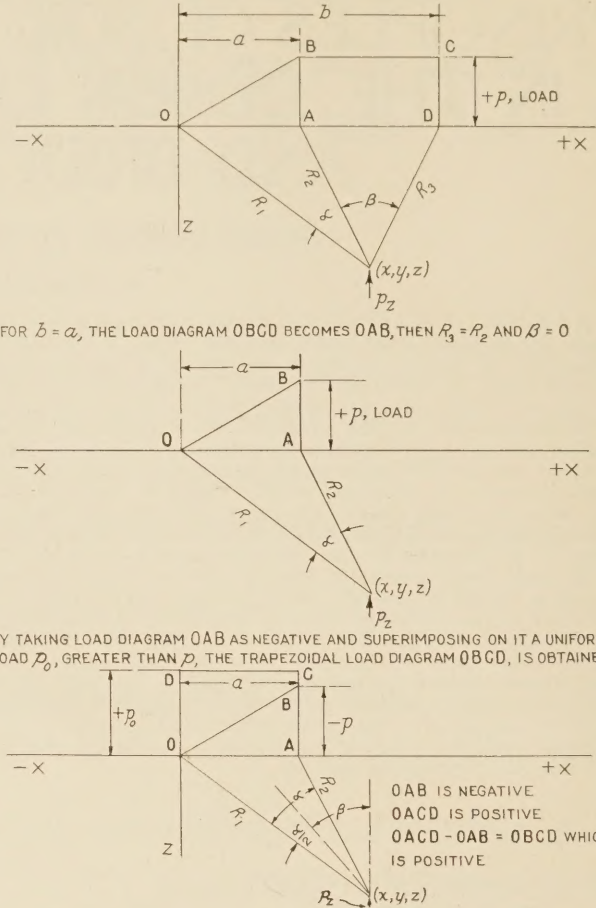


FIGURE 2.—DEVELOPMENT OF DIAGRAM SHOWING STRIP TRAPEZOIDAL LOAD DISTRIBUTION OVER A LONG STRIP.

fig. 1). The loads are infinite in extent in both the X and Y directions, the Y direction being perpendicular to the plane of the figure.

2. By first taking $b=a$ in the upper diagram, $OBCD$, of figure 2, there is obtained a system of triangular loading, OAB , over a long strip as indicated. If this triangular load is then given a negative sign, and there is then superimposed on it a strip of uniform pressure, p_0 , as shown in the lower diagram, there results a trapezoidal load distribution, $OBCD$, over a long strip.

Example 1—Derivation of formulas for stresses beneath a fill.—In problems of plane strain it is usually sufficient to know six stresses: The normal stresses, p_x and p_z , acting in the directions of the OX and OZ axes, respectively; the principal stresses, p_1 and p_2 , acting at right angles to each other and perpendicular to planes of zero shearing stress; the shearing stress, s_{xz} , corresponding to the normal stresses, p_x and p_z ; and the maximum shearing stress, s_{max} , at any point, equal in magnitude to half the difference of the two principal stresses at that point. That is, at any point (x, y, z) in the stressed undersoil,

$$s_{max} = \frac{p_1 - p_2}{2} \dots \dots \dots (1)$$

where p_1 is the major and p_2 the minor principal stress. Since displacements in the undersoil in the direction of the OY axis (perpendicular to the XOZ plane) are zero, it is usually unnecessary to consider the normal stress, p_y , acting in this direction. It is necessary, however, to consider the magnitude of p_y at the terminal of a long loaded strip or fill where the retaining wall or abutment is placed. In computing p_1 , p_2 , and s_{max} , p_y is not

needed in problems of plane strain. In texts³ dealing with the theory of elasticity, the following relations are derived:

$$p_1 = \frac{p_x + p_z}{2} + \left[\left(\frac{p_x - p_z}{2} \right)^2 + (s_{xz})^2 \right]^{1/2} \quad (2)$$

$$p_2 = \frac{p_x + p_z}{2} - \left[\left(\frac{p_x - p_z}{2} \right)^2 + (s_{xz})^2 \right]^{1/2} \quad (3)$$

$$s_{\max.} = \frac{p_1 - p_2}{2} = \left[\left(\frac{p_x - p_z}{2} \right)^2 + (s_{xz})^2 \right]^{1/2} \quad (4)$$

Hence, if at any point (x, y, z) of the undersoil, the stresses, p_x , p_z , and s_{xz} , are known, values for p_1 , p_2 , and $s_{\max.}$ are easily derived.

ISOSHEAR LINES DETERMINED FOR MATERIAL BENEATH A FILL

With reference to the load diagram for a cut in figure 1, the vertical pressure, p_z , at a point (x, y, z) in the undersoil as derived by Carothers was found to be

$$p_z \text{ (for cut)} = \frac{p}{\pi a} [\pi a - a(\alpha_1 + \alpha_2 + \alpha_3) - b(\alpha_1 + \alpha_3) - x(\alpha_1 - \alpha_3)] \quad (5)$$

Formula (5) as written is for compression. If p is given a negative sign, then p_z is tension. If a uniform compression, p , is added to this tension, i. e., if the expression on the right of formula (5) is subtracted from p , there results the formula for the vertical pressure, p_z , at the same point as produced by the load diagram for a fill, figure 3. That is,

$$p_z \text{ (for fill)} = p - \frac{p}{\pi a} [\pi a - a(\alpha_1 + \alpha_2 + \alpha_3) - b(\alpha_1 + \alpha_3) - x(\alpha_1 - \alpha_3)]$$

or

$$p_z \text{ (for fill, fig. 3)} = \frac{p}{\pi a} [a(\alpha_1 + \alpha_2 + \alpha_3) + b(\alpha_1 + \alpha_3) + x(\alpha_1 - \alpha_3)] \quad (6)$$

where the angles, α_1 , α_2 , and α_3 , are expressed in radians.

Similarly, by taking Carothers' formulas for p_x and s_{xz} for the cut and considering p_x and s_{xz} as produced by the uniform compression as p and zero, respectively, there is obtained

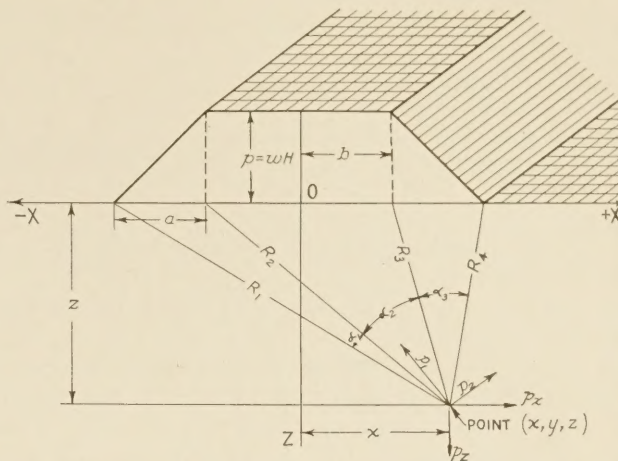
$$p_x \text{ (for fill)} = \frac{p}{\pi a} \left[a(\alpha_1 + \alpha_2 + \alpha_3) + b(\alpha_1 + \alpha_3) + x(\alpha_1 - \alpha_3) - 2z \log_e \frac{R_1 R_4}{R_2 R_3} \right] \quad (7)$$

and

$$s_{xz} = -\frac{zp}{\pi a} (\alpha_1 - \alpha_3) \quad (8)$$

By substituting the values for p_z , p_x , and s_{xz} , as given in formulas (6), (7), and (8), in formulas (2), (3), and (4), expressions for the stresses, p_1 , p_2 , and $s_{\max.}$, are obtained. Thus

$$s_{\max.} = \frac{zp}{\pi a} \left[\log_e^2 \frac{R_1 R_4}{R_2 R_3} + (\alpha_1 - \alpha_3)^2 \right]^{1/2} \quad (9)$$



$$p_z = \frac{p}{\pi a} [a(\alpha_1 + \alpha_2 + \alpha_3) + b(\alpha_1 + \alpha_3) + x(\alpha_1 - \alpha_3)]$$

$$p_x = \frac{p}{\pi a} \left[a(\alpha_1 + \alpha_2 + \alpha_3) + b(\alpha_1 + \alpha_3) + x(\alpha_1 - \alpha_3) - 2z \log_e \frac{R_1 R_4}{R_2 R_3} \right]$$

$$s_{xz} = -\frac{zp}{\pi a} (\alpha_1 - \alpha_3)$$

$$p_1 = \frac{p}{\pi a} \left[a(\alpha_1 + \alpha_2 + \alpha_3) + b(\alpha_1 + \alpha_3) + x(\alpha_1 - \alpha_3) - z \log_e \frac{R_1 R_4}{R_2 R_3} \right] + \frac{zp}{\pi a} \sqrt{\log_e^2 \frac{R_1 R_4}{R_2 R_3} + (\alpha_1 - \alpha_3)^2}$$

$$p_2 = \frac{p}{\pi a} \left[a(\alpha_1 + \alpha_2 + \alpha_3) + b(\alpha_1 + \alpha_3) + x(\alpha_1 - \alpha_3) - z \log_e \frac{R_1 R_4}{R_2 R_3} \right] - \frac{zp}{\pi a} \sqrt{\log_e^2 \frac{R_1 R_4}{R_2 R_3} + (\alpha_1 - \alpha_3)^2}$$

$$s_{\max.} = \frac{zp}{\pi a} \sqrt{\log_e^2 \frac{R_1 R_4}{R_2 R_3} + (\alpha_1 - \alpha_3)^2}$$

FIGURE 3.—LOAD DIAGRAM AND COMPUTATION OF STRESSES IN EARTH BELOW A FILL.

Along the axis, OZ , $R_1 = R_4$, $R_2 = R_3$, and $\alpha_1 = \alpha_3$. Hence formula (9) reduces to

$$s_{\max.} = \frac{zp}{\pi a} \log_e \left[\frac{R_1}{R_2} \right]^2 = \frac{2zp}{\pi a} \log_e \frac{R_1}{R_2} \quad (10)$$

For $a=b$, figure 3, and for points along OZ , it is found by trial that the greatest value of $s_{\max.}$ is at the point, $z = \frac{3}{2}a$, where $s_{\max.} = 0.31p$ (or $0.3p$ approximately)

Similarly, by taking $a=2b$, the greatest value of $s_{\max.}$ at any point on the center line, OZ , is at $z=0.96a$, where $s_{\max.} = 0.30p$. It is worthy of note that these relations are independent of the height, H , of the fill.

By varying the height and the slope, and keeping $\frac{a}{b}$

same, the relation, greatest $s_{\max.} = 0.3p$ at $z = \frac{3}{2}a$ for $a=b$ or at $z=0.96a$ for $a=2b$, is not changed, although the magnitude of p and therefore, of $s_{\max.}$, increases as H is increased. Here $p=wH$, where w is the average unit weight of fill material.

By drawing accurately and to scale the load diagram, the radial lines, R_1 , R_2 , R_3 , and R_4 , the vertical and

³ See, for example, pp. 16 to 19, inclusive, of Theory of Elasticity, by S. Timoshenko. McGraw-Hill Book Co., 1934.

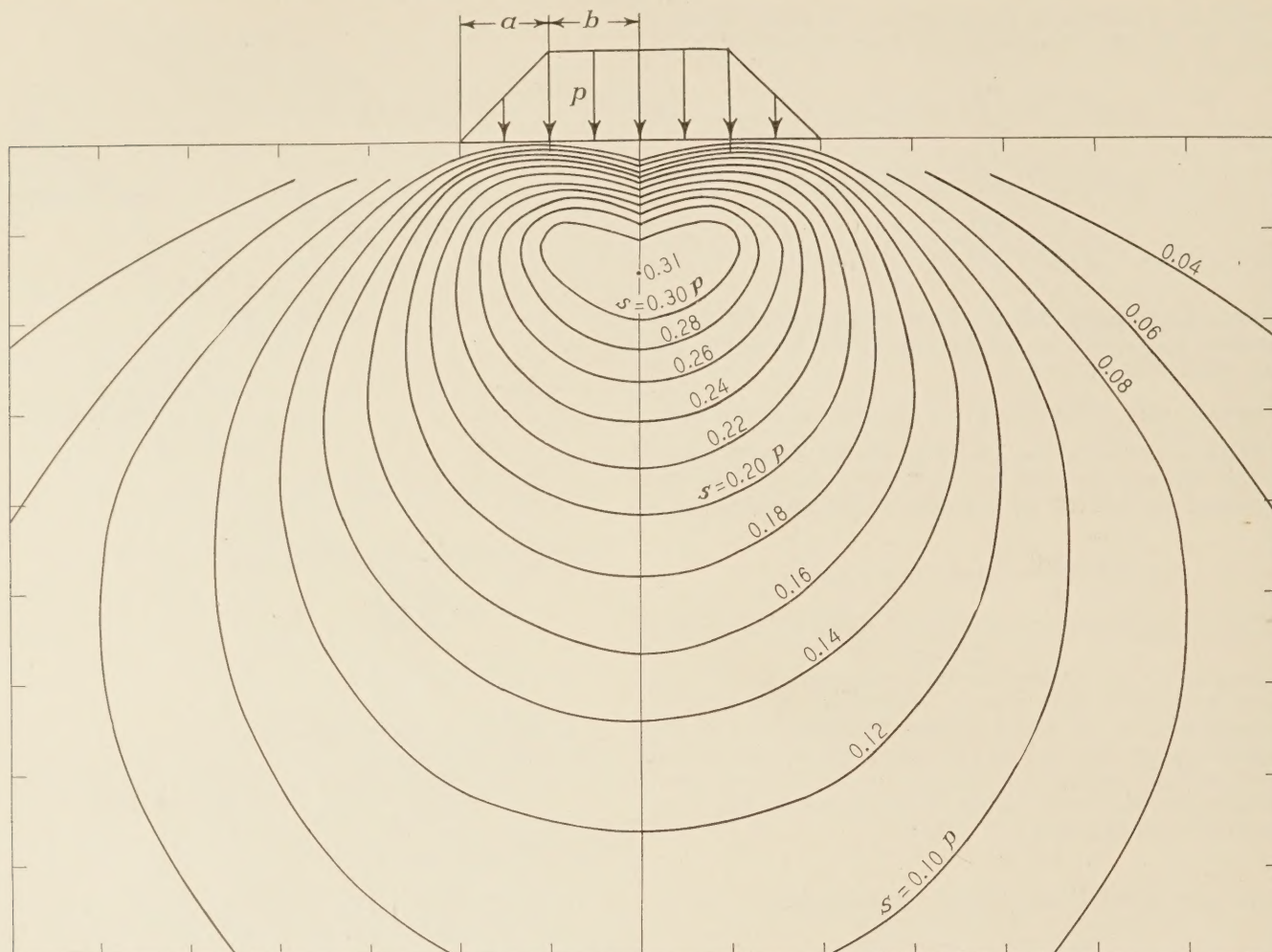


FIGURE 4.—ISOSHEAR LINES UNDER TYPICAL FILL, WHERE $a=b$.

horizontal distances z and x , respectively, and the subtended angles, α_1 , α_2 , and α_3 , the numerical values of s_{\max} , may be computed for various points in the supporting soil. All points of the same s_{\max} may be connected by a smooth curve, and a series of such curves or isoshear lines, as shown in figure 4, may be drawn.

It has been shown⁴ that if the greatest value of s_{\max} , namely $0.3p$, does not exceed the unit cohesion (of the undersoil), the supporting power of the undersoil is usually ample, and that if $0.3p$ exceeds the unit cohesion, a further analysis of the supporting power of the undersoil should be made.

If $0.3p$ exceeds the unit cohesion c of the undersoil, it does not follow that failure of the supporting earth is inevitable, but it is necessary in such a case to determine the supporting power q by Prandtl's formula,⁵ which is

$$q = (c \cot \phi + wb' \cot \alpha) \left[\frac{1 + \sin \phi}{1 - \sin \phi} e^{\pi \tan \phi} - 1 \right]$$

where, with respect to the supporting soil,

q = supporting power,
 c = the unit cohesion,

ϕ = the angle of internal friction,

w = unit weight of undersoil,

$b' = \frac{a}{2} + b$ (see figs. 3 and 4), and

$\alpha = 45^\circ - \phi/2$.

SAMPLE CALCULATION OF SUPPORTING POWER GIVEN

As an example, suppose that q is to be determined for the supporting soil beneath a fill in which the dimension $a=b=20$ feet and which has a height of 20 feet, giving a value for $p=2,000$ pounds per square foot, the unit weight of fill material being 100 pounds per cubic foot. Suppose that the values c and ϕ for the supporting soil are 200 pounds per square foot and 5° , respectively. This value for c is less than $0.3 \times 2,000 = 600$ pounds per square foot. The value of α is $45^\circ - \frac{5^\circ}{2} = 42.5^\circ$ and $\cot \alpha = 1.091$. Assume that w for the undersoil is 100 pounds per cubic foot. The value $\cot 5^\circ = 11.43$, $\sin \phi = 0.087$ and $\tan \phi = 0.0875$. Then by substitution in Prandtl's formula,

$$q = (200 \times 11.43 + 100 \times 30 \times 1.091) \left[\frac{1 + 0.087}{1 - 0.087} e^{\pi \times 0.0875} - 1 \right] \\ = 3,150 \text{ pounds per square foot.}$$

The factor of safety against complete failure of the supporting soil is

⁴ Principles of Soil Mechanics Involved in Fill Construction, by L. A. Palmer and E. S. Barber, Proceedings of the Highway Research Board, Annual Meeting, 1937.

⁵ Prandtl's formula as originally derived pertains to uniform strip loading. The formula is adapted to the case of trapezoidal loading (fill) by reconstruction of the load diagram, changing the trapezoid (fig. 3) to a rectangle of equal area.

$$F = \frac{q}{p} = \frac{3,150}{2,000} = 1.6.$$

The approximate working rule, that $0.3p$ should not exceed the unit cohesion c of the supporting soil, does not take into account the frictional resistance of the undersoil and the resistance offered by the weight of the displaced undersoil when it fails. Prandtl's formula takes these factors into account. This approximate rule is usually well on the side of safety against ultimate failure if ϕ is greater than 10° and if the ground-water level is considerably below the surface of the supporting soil. Buoyancy produced by ground water diminishes the value of w in Prandtl's formula.

Only ultimate failure of the supporting soil is considered in the preceding example. It is entirely possible that even with a factor of safety of as much as 2 against ultimate failure, there may nevertheless be displacement of the undersoil to an extent such that the fill settles beyond the maximum allowable amount, and in this event it would be necessary to have a much higher factor of safety than 2. If a correlation between displacements of large soil masses on the one hand and deformations in laboratory samples on the other were obtained, it should be possible to take a laboratory value c' (rather than the ultimate value c) corresponding to the maximum allowable deformation in the supporting soil and refer the factor of safety to this value.

Example 2—Derivation of formulas for stresses beneath a trapezoidal load distribution.—With reference to the upper load diagram, *OBCD*, figure 2, Carothers has derived the formulas for stresses at any point (x, y, z) of the undersoil. For p_z at any point he obtains:

$$p_z = \frac{p}{\pi a} \left[a\beta + x\alpha - \frac{az}{R_3^2}(x-b) \right] \dots\dots\dots (11)$$

If $b=a$, angle $\beta=0$, $R_3=R_2$, and formula (11) reduces to

$$p_z = \frac{p}{\pi a} \left[x\alpha - \frac{az}{R_2^2}(x-a) \right] \dots\dots\dots (12)$$

which is the value of p_z at any point (x, y, z) in the undersoil beneath a triangular load (*OAB*, center diagram fig. 2) extending over a long distance in the Y direction. If p is now given a negative sign in formula (12), p_z becomes negative at the point. If, now, a strip of uniform pressure, p_0 , is superimposed on the negative triangular load, *OAB* (see lower diagram of fig. 2), it is possible to derive the expression for p_z at the point (x, y, z) as produced by the trapezoidal load, *OBCD*. Thus, for the uniform pressure, p_0 , over the strip of width a and represented by the load diagram *OACD*, lower diagram of figure 2,

$$p_z = \frac{p_0}{\pi a} (a\alpha + a \sin \alpha \cos 2\beta) \dots\dots\dots (13)$$

If the expression on the right of formula (12) is now subtracted from the expression on the right of formula (13), there results,

$$p_z = \frac{p_0}{\pi a} (a\alpha + a \sin \alpha \cos 2\beta) - \frac{p}{\pi a} \left[x\alpha - \frac{az}{R_2^2}(x-a) \right] \dots\dots (14)$$

which is the expression for p_z at any point (x, y, z) in the undersoil resulting from the trapezoidal load, *OBCD*, at the surface. In a similar manner it is found that

$$p_x = \frac{p_0}{\pi a} (a\alpha - a \sin \alpha \cos 2\beta) - \frac{p}{\pi a} \left[x\alpha + \frac{az}{R_2^2}(x-a) + 2z \log_e \frac{R_2}{R_1} \right] \dots\dots\dots (15)$$

$$s_{zz} = \frac{p_0}{\pi a} (a \sin \alpha \sin 2\beta) + \frac{p}{\pi a} \left[z\alpha - a \frac{z^2}{R_2^2} \right] \dots\dots (16)$$

and

$$s_{\max} = \frac{1}{\pi a} \left\{ p_0 a \sin \alpha \cos 2\beta + p \frac{az}{R_2^2}(x-a) + p_z \log_e \frac{R_2}{R_1} \right\}^2 + \left[p_0 a \sin \alpha \sin 2\beta + p \left(z\alpha - a \frac{z^2}{R_2^2} \right) \right]^2 \dots\dots\dots (17)$$

By substitution of various values for $\alpha, \beta, R_1, R_2, x$, and z in formula (17), it is found that the greatest value of s_{\max} is found at the point *O*, figure 5, and that this value is equal to $\frac{p_0}{\pi}$ where p_0 is the maximum applied pressure.

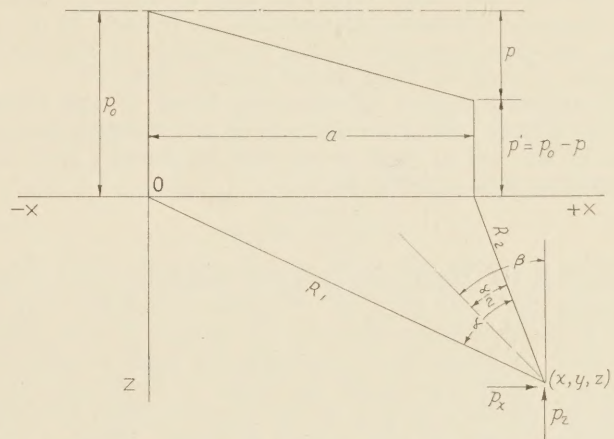


FIGURE 5.—TRAPEZOIDAL LOAD DISTRIBUTION DIAGRAM. SEE FORMULAS (14), (15), (16), AND (17).

CONSIDERATION GIVEN TO EARTH PRESSURES TENDING TO PRODUCE ROTATING MOMENT

A trapezoidal load distribution, as illustrated in figure 5, results whenever a rotating moment is applied to a retaining wall or abutment, and in this figure the point, *O*, may be considered as at the toe. There is no danger of failure of the undersoil if the cohesion of the supporting soil corresponding to the maximum allowable movement of the wall or abutment exceeds $\frac{p_0}{\pi}$. If the cohesion is less than this greatest shearing stress, it does not follow that failure of the undersoil will result although a plastic region at the toe is likely to be developed, and in this case the stress relations as given by formulas (14), (15), (16), and (17) no longer apply. The whole system of stress distribution is then changed. Prior to further consideration of this subject, it is necessary to consider the earth pressures tending to produce the rotating moment.

There are two principal kinds of soil deformation caused by load: (1) Volume change; and (2) distortion resulting from shear. Volume change results when a compressible soil stratum is consolidated by causing water to escape from the stratum under pressure into one or more permeable strata (drainage courses) bounding the compressible soil layer. On the other hand, it is assumed that distortion alone produces no volume change in a soil. One of the basic principles

of soil mechanics has been that a soil maintained at a constant moisture content is incompressible. This could be true, of course, if the voids are completely filled with water and if each individual soil particle is assumed to be capable of a change in shape but not in volume, in which case the value of Poisson's ratio would be $\frac{1}{2}$.

The magnitude of distortion caused by shearing stresses depends on the magnitude of the stresses and the shearing resistance of the soil. It may proceed slowly and cause a slow subsidence of the supporting soil, or it may occur very quickly as in a landslide. The relatively slow displacement may cause failure of the structure without developing a surface of failure or shear in the supporting soil. The allowable deformation depends on the structure, and it may be considerably less than the magnitude of the deformation or distortion that is characteristic of the yield value or ultimate shearing resistance of the soil. Laboratory tests can provide the design engineer with a complete shearing stress-deformation relationship for the soil in question, and this, together with a knowledge of the earth stresses, should be very useful information.

At ultimate failure the shearing stress at any point on the surface of failure is equal to the shearing resistance of the soil at that point, and Coulomb's formula expressing this equality is

$$s = c + p_n \tan \phi \text{-----} (18)$$

where s is the total unit shearing resistance and c the cohesion per unit of area. Cohesion may be only a part of the shearing resistance. If friction is developed, the other part is $p_n \tan \phi$ where ϕ is the angle of internal friction (limiting value of the angle of obliquity) and p_n is the pressure normal to the tangent plane through any given point on the surface of shear. Both c and ϕ are limiting values in this formula, that is, they are values which obtain at the instant of sudden and complete failure of the earth mass.

If the shearing stress in the soil mass equals half the shearing resistance, s , then the factor of safety insofar as the soil is concerned is 2. However, for the structure supported by this soil mass, this number may be meaningless, c and ϕ being ultimate values, and it is preferable to take values of c and ϕ that correspond to the maximum allowable soil deformation for the particular structure. In formula (18) it is assumed that the normal pressure p_n is transmitted solely from grain to grain of soil and that no part of p_n is hydrostatic pressure. The conditions that exist when a portion of p_n is carried by water have been analyzed by Terzaghi.⁶

MOHR'S GRAPHICAL METHOD USEFUL IN PROBLEMS OF PLANE STRAIN

For any material in which ϕ is zero, the shearing strength is not increased by pressure. Thus, a cylindrical specimen of such material, subjected to a load in the direction of its axis, would have theoretically the same shearing strength for a lateral (hydraulic) pressure of zero as for one of considerable magnitude. If ϕ is not zero, the shearing strength increases with increasing lateral pressure, p_n . In a cylinder of homogeneous material, the displacements in any two or more different vertical planes through the longitudinal axis are

⁶ The Shearing Resistance of Saturated Soils and the Angle between the Planes of Shear, by Dr. Charles Terzaghi, vol. I, pp. 54 to 66, inclusive, Proceedings of the International Conference on Soil Mechanics and Foundation Engineering, 1936.

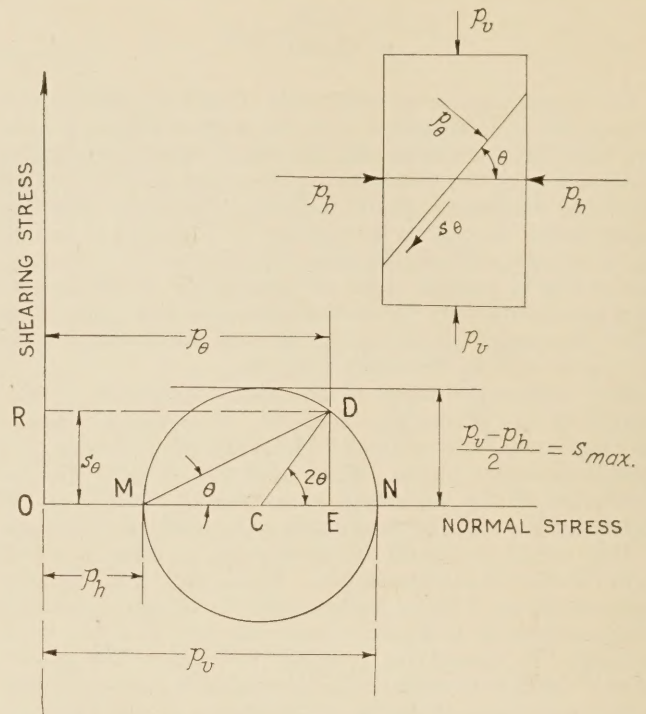


FIGURE 6.—GRAPHICAL ANALYSIS OF STRESSES IN A COMPRESSED CYLINDER, USING MOHR'S CIRCLE OF STRESS.

the same. Points in any such vertical plane remain in that plane during the period of stress. Hence, the compressed cylinder is treated as though it were another case of plane strain. For a graphical analysis of the stresses in such a system, Mohr's diagram is very useful. The graphical method is illustrated in its simplest form in figure 6, and the following procedure enables one to compute the normal stress, p_θ , and the shearing stress, s_θ , for any plane, θ , through the stressed cylinder, p_v and p_h being the only applied stresses.

Procedure for computing p_θ and s_θ .—

1. On the normal stress axis, figure 6, lay off to scale the distances, OM and ON , proportional to p_h and p_v , respectively.

2. Draw a circle around the diameter, MN .

3. The normal stresses, p_v and p_h , are principal stresses. There are no shearing stresses on the planes (principal planes) to which these stresses are perpendicular. The maximum ordinate to any point on the circle is the radius of the circle. The diameter $= MN = p_v - p_h$, and the radius is $\frac{p_v - p_h}{2} = s_{max}$.

4. A line drawn from M to any point, D , on the circle represents a plane through the center of the cylinder, inclined at an angle, θ , with the horizontal. There are an infinite number of planes through the center of the cylinder and a corresponding infinite number of points on the circle. The normal stress on the plane, θ , through the cylinder is the horizontal distance, RD , in the stress diagram,

$$RD = OE = OM + MC + CE = OM + MC + CD \cos 2\theta$$

$$= p_h + \frac{p_v - p_h}{2} + \left[\frac{p_v - p_h}{2} \right] \cos 2\theta$$

Hence

$$p_\theta = \frac{p_h + p_v}{2} + \left[\frac{p_v - p_h}{2} \right] \cos 2\theta \text{-----} (19)$$

For $\theta=0$, $p_\theta=p_v$ and for $\theta=45^\circ$, $p_\theta=OC=\frac{p_v+p_h}{2}$. For $\theta=90^\circ$, $p_\theta=p_h$.

5. The shearing stress, s_θ , on the plane, θ , is the ordinate value, DE . That is,

$$s_\theta = DE = CD \sin 2\theta$$

or

$$s_\theta = \left[\frac{p_v - p_h}{2} \right] \sin 2\theta \quad \text{----- (20)}$$

For $\theta=45^\circ$, s_θ is a maximum and equal to $\frac{p_v - p_h}{2}$. For $\theta=90^\circ$, $s_\theta=0$ and for $\theta=0$, $s_\theta=0$. Hence on the two mutually perpendicular planes, $\theta=0$ and $\theta=90^\circ$, there is no shearing stress, p_v being perpendicular to $\theta=0$ and p_h to $\theta=90^\circ$.

PLANE WHERE SHEARING RESISTANCE EQUALS SHEARING STRESS DETERMINED GRAPHICALLY

In the stressed cylinder, p_v is the same on all horizontal planes and p_h is the same on all vertical planes. Hence p_θ and s_θ have constant values on one and the same plane. This condition does not exist in an earth mass where the principal normal stresses vary both in direction and magnitude from one point to another. Hence in an earth mass the Mohr's diagram must be considered with reference to stresses all in the immediate neighborhood of a particular point.

The graphical procedure above described is with reference to stress and without regard to the resistance of the material to stress; and no elastic constants are considered, since the problem is one of plane strain. If the angle, ϕ , characteristic of the material, is not zero and if a cylinder of the material fails in shear under a compression, p_v , and a lateral pressure, p_h , then if p_h is increased to p_h' , the compressive strength, p_v , will be increased correspondingly to a value, p_v' . This condition may be represented by two stress circles (see fig. 7), the first having a diameter equal to $p_v - p_h$ and the second a diameter equal to $p_v' - p_h'$. In both instances, failure occurs theoretically on that plane, θ , where the shearing resistance equals the shearing stress according to formula (18). The graphical procedure of determining this plane is as follows (see fig. 7):

1. Describe circles around the diameters, $p_v - p_h$ and $p_v' - p_h'$. The distances, OM and OM' , represent p_h and p_h' , respectively.

2. Draw a straight line tangent to both circles. Draw the lines, MT and $M'T'$, to the points of tangency. These two lines represent the most dangerous planes and are called the planes of failure. Both are inclined at the same angle, α , with the horizontal.

3. The tangent line called "Mohr's envelope" is inclined at the angle, ϕ , to the horizontal. Its equation is formula (18),

$$s = c + p_n \tan \phi,$$

c and ϕ being ultimate values. At the origin, $p_n=0$ and the shearing resistance at zero normal pressure equals the cohesion, c . The intercept of the envelope line with the shearing stress axis is c and its slope is $\tan \phi$.

From geometry, $2\alpha = 90^\circ + \phi$ or $\alpha = 45^\circ + \frac{\phi}{2}$. If the material is such that $\phi=0$, the most dangerous planes are inclined at 45° to the horizontal.

4. The shearing stress on any plane, for example the plane, $M'D$ on the larger circle, is obtained from for-

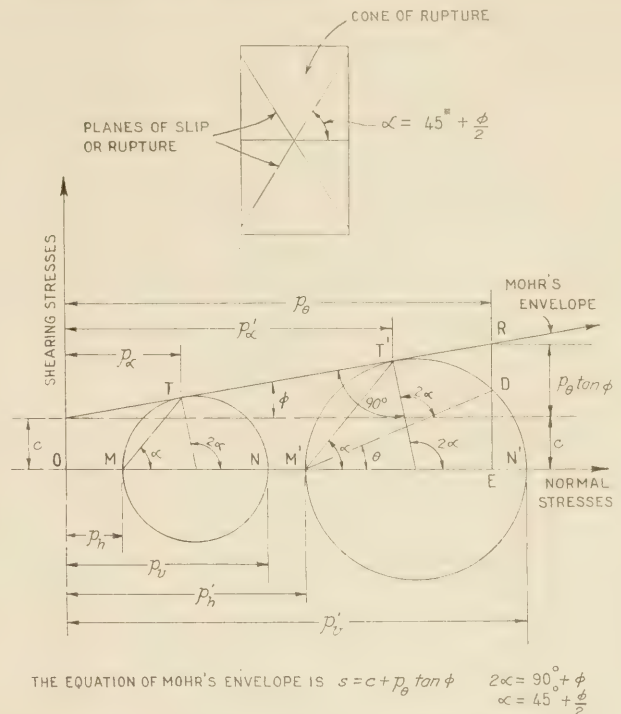


FIGURE 7.—GRAPHICAL ANALYSIS FOR DETERMINING PLANE OF FAILURE.

mula (20). On the plane, $M'D$, the shearing stress is the ordinate ED , and the shearing resistance on this plane is $ER = c + p_\theta \tan \phi$ where p_θ is the pressure normal to the plane, $M'D$. The shearing resistance is greater than the shearing stress on this plane, and this condition exists on all planes except the most dangerous ones, where, according to Mohr's theory, the shearing stress equals the shearing resistance. On the plane, $M'T'$, the shearing resistance, s , is equal to $c + p'a \tan \phi$.

In accordance with this theory, failure may be by fracture, as in the crushing of a concrete cylinder, or it may be evidenced by plastic flow, in which case the dangerous planes are planes of "slip" or flow. When plastic yield occurs, helical slip lines (Lüders lines) are often visible on the exterior surface of the cylinder. Visual observations of Lüders lines and fractured surfaces in stressed cylinders of homogeneous materials tend generally to substantiate Mohr's theory, which is essentially a graphical representation of Coulomb's law, formula (18).

EARTH PRESSURES COMPUTED WITH THE AID OF MOHR'S THEORY

It has been previously indicated in this paper that in considering the supporting power of soils conservative values for cohesion and friction (that is, values less than the ultimate) should be taken. Thus the unit cohesion of the undersoil below a fill should not be exceeded by the greatest shearing stress, the unit cohesion in this case being that corresponding to the maximum allowable deformation and therefore less than the ultimate value, symbolized by the letter, c . In the development of Mohr's theory of failure and Coulomb's formula only the ultimate values, c and ϕ , are considered.

There are instances, however, when it is on the side of safety to use only the ultimate values, c and ϕ , in computations. An example is the computation of passive earth pressure against an abutment or retaining wall. The formula for the passive earth pressure is

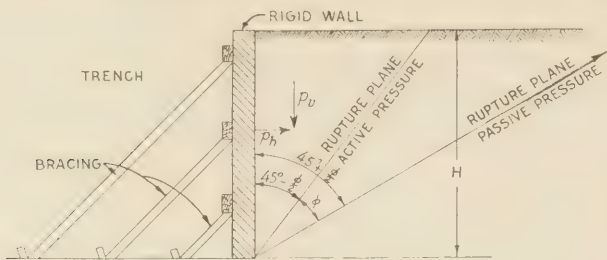


FIGURE 8.—SCHEMATIC DIAGRAM SHOWING EARTH MASS, RETAINING WALL, AND RUPTURE PLANES.

$$p \text{ (passive)} = p_1 \tan^2 \left(45^\circ + \frac{\phi}{2} \right) + 2c \tan \left(45^\circ + \frac{\phi}{2} \right)$$

where p (passive) and p_1 are principal stresses. It is not safe to underestimate the magnitude of p (passive), which, as seen in this formula, increases as c and ϕ increase and which is produced by the expansion of soil back of a retaining wall. This formula and the one for active earth pressure are developed by the following procedure.

Consider a level earth mass of cohesive and homogeneous soil of great depth and extent. It is assumed that it is possible to cut out a trench of given depth and of great length in the soil mass without any disturbance of the remaining earth. It is next supposed that a rigid wall with bracing is erected (still without disturbing the soil) along the entire length of a side of the perpendicular embankment (see fig. 8). The unit weight of earth is taken as w and if the vertical distance from the surface to a small element of earth touching the wall is H' , then the vertical pressure, p_v , on the element equals wH' , assuming zero friction between earth and wall. To this vertical pressure there corresponds a horizontal pressure, p_h , and it is assumed that the values, p_v and p_h , have remained unchanged during the construction of the rigid wall and bracing.

If the wall remains unyielding, the ratio, $\frac{p_h}{p_v}$, is known as the coefficient of earth pressure at rest. In figure 9, the stresses on the element adjacent to the wall and at a depth, H' , are represented by circle (1), the circle for earth pressure at rest. It is assumed that the stresses are transmitted solely from grain to grain of soil. Terzaghi⁷ has estimated the coefficient of earth pressure at rest as being within the limits, 0.70 to 0.75, in cohesive soils and ranging from 0.40 to 0.45 in sands. Various authors have expressed doubt as to the constancy of this ratio throughout a considerable depth of homogeneous soil. With reference to figure 8, where for the unyield-

ing wall $\frac{p_h}{p_v} = K$, a constant, the total pressure against a vertical strip of unit width of the wall is $P_h = \frac{K p_v H}{2}$

where H is the height of the wall. If $K=0.70$, $H=20$ feet, and $w=100$ pounds per cubic foot, then

$$P_h = \frac{K w H^2}{2} = \frac{0.7 \times 100 \times 400}{2} = 14,000 \text{ pounds.}$$

SAMPLE CALCULATIONS OF EARTH PRESSURES GIVEN

Now assume that the wall yields and moves outward to an extent such that the soil mass back of it fails suddenly in shear. The weight of earth and therefore the

⁷ A Fundamental Fallacy in Earth Pressure Computations, by Charles Terzaghi, publications from the Graduate School of Engineering, Harvard University, 1935-36, No. 182, Soil Mechanics Series No. 3.

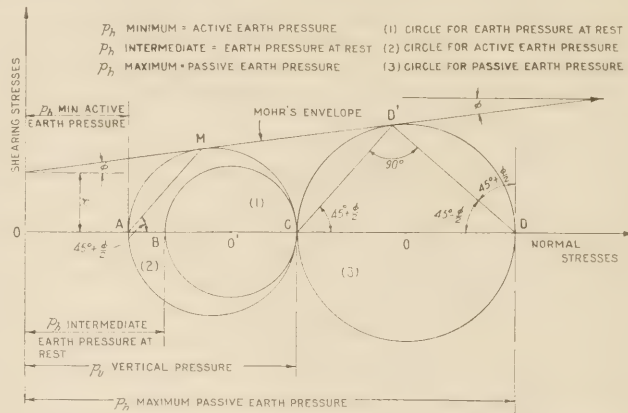


FIGURE 9.—DIAGRAMS SHOWING ACTIVE AND PASSIVE EARTH PRESSURES AND EARTH PRESSURE AT REST.

value of p_v at any point along the wall are constant during this occurrence, but (fig. 9) the stress circle has grown and become tangent to the rupture line (Mohr's envelope). This has occurred by reason of a diminution in p_h and, with p_v constant, the diameter of the circle has increased from $p_v - p_h$ intermediate to $p_v - p_h$ minimum, and

$$p_h \text{ int.} = \text{earth pressure at rest,}$$

and

$$p_h \text{ min.} = \text{active earth pressure.}$$

Failure occurs along the surface AM (fig. 9), inclined at $45^\circ + \frac{\phi}{2}$ to the horizontal or $45^\circ - \frac{\phi}{2}$ to the vertical.

On the other hand, assume that enough lateral pressure is applied against the wall from the excavated side to cause the earth to shear and be displaced upward. The lateral pressure required to effect this displacement is equal to the passive earth pressure, $p_h \text{ max.}$ (see fig. 9). The magnitude of this pressure is denoted by the distance, OD , and failure occurs along a plane inclined at $45^\circ + \frac{\phi}{2}$ to the vertical (DD' , fig. 9).

The stress circles, (2) and (3) of figure 9, for the active and passive earth pressures, respectively, are redrawn in figure 10. It is then seen that in circle (2),

$$\cos \phi = \frac{O'M}{O'L} = \frac{p_v - p_h \text{ min.}}{O'B + BL} = \frac{p_v - p_h \text{ min.}}{c + \left[\frac{p_v + p_h \text{ min.}}{2} \right] \tan \phi.}$$

Then

$$\frac{p_h \text{ min.}}{p_v} = \frac{1 - \sin \phi}{1 + \sin \phi} - \frac{2c \cos \phi}{(1 + \sin \phi) p_v}$$

and hence

$$p_h \text{ min.} = p_v \tan^2 \left(45^\circ - \frac{\phi}{2} \right) - 2c \tan \left(45^\circ - \frac{\phi}{2} \right) \dots (21)$$

With reference to circle (3), figure 10, it is evident that the relationship of p_v to $p_h \text{ max.}$ is the same as that of $p_h \text{ min.}$ to p_v , that is,

$$p_v = p_h \text{ max.} \tan^2 \left(45^\circ - \frac{\phi}{2} \right) - 2c \tan \left(45^\circ - \frac{\phi}{2} \right)$$

or

$$p_h \text{ max.} = \frac{p_v}{\tan^2 \left(45^\circ - \frac{\phi}{2} \right)} + \frac{2c}{\tan \left(45^\circ - \frac{\phi}{2} \right)}$$

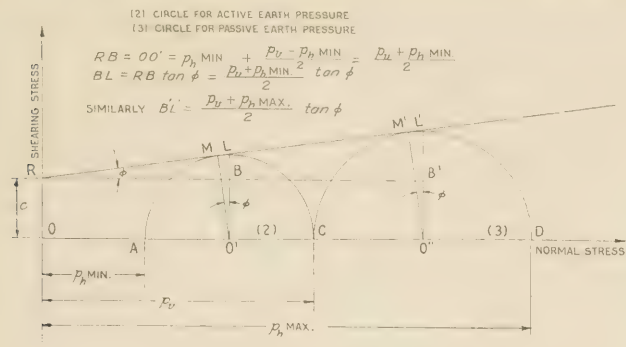


FIGURE 10.—DIAGRAMS SHOWING ACTIVE AND PASSIVE EARTH PRESSURES.

and hence

$$p_h \text{ max.} = p_v \tan^2 \left(45^\circ + \frac{\phi}{2} \right) + 2c \tan \left(45^\circ + \frac{\phi}{2} \right) \dots (22)$$

Take $c=200$ pounds per square foot and $\phi=20^\circ$ with reference to the illustration, figure 8, then

$$p_h \text{ min.} = 0.490 p_v - 280 \text{ pounds per square foot,}$$

and

$$p_h \text{ max.} = 2.039 p_v + 571 \text{ pounds per square foot.}$$

For $w=100$ pounds and $H=20$ feet, the average p_v will be 1,000 pounds per square foot. Then, in summary, the total forces exerted against the wall by earth pressure at rest, active earth pressure, and passive earth pressure are:

Total lateral pressure on 1-foot vertical strip of wall

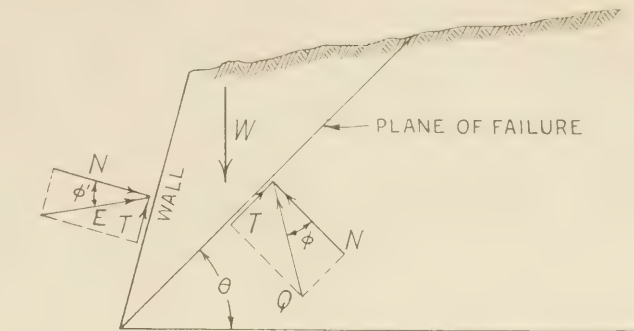
- For earth pressure at rest... $0.7 \times 1,000 \times 20 = 14,000$ pounds.
- For active earth pressure... $(490 - 280) \times 20 = 4,200$ pounds.
- For passive earth pressure... $(2,039 + 571) \times 20 = 52,200$ pounds.

Terzaghi⁸ has shown that passive earth pressure may be exerted by clay soils against retaining walls. Such soils tend to expand and shrink noticeably, according to seasonal climatic variations. Hence, walls strong enough to withstand the pressure of a cohesionless backfill are gradually and intermittently pushed out of plumb by the swelling of a cohesive clay soil, characterized by low permeability and appreciable volume changes on wetting and drying. On swelling, the backfill exerts passive earth pressure against the wall.

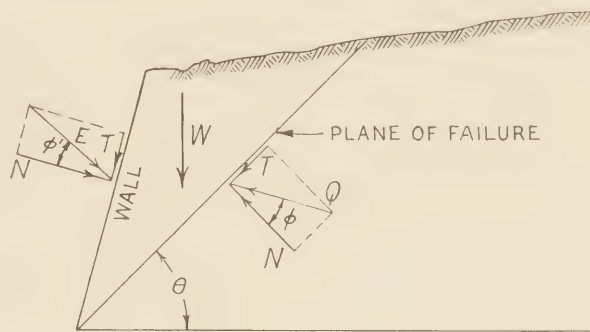
In the foregoing discussion and with reference to figures 8 and 9, the wall was assumed as vertical and parallel in direction to the principal plane to which p_h is normal. The surface of the backfill being level with the top of the wall and the friction between the wall and backfill material being taken as zero, there is no difficulty in locating the planes of failure for active and passive earth pressures. In both cases the resultant earth pressure (usually designated as E) is located at one-third the distance upward from the bottom of the cut, assuming that p_v increases directly with depth.

SHEARING PLANE DETERMINED BY GRAPHICAL METHODS

For the more general case the surface of the backfill is not level; there is a certain amount of friction between the backfill material and the wall; the wall is not parallel to a principal plane; and the force exerted against the wall is not horizontal. The analysis of the general



ACTIVE EARTH PRESSURE



PASSIVE EARTH PRESSURE

N = NORMAL FORCE, T = FRICTIONAL FORCE
 AND E AND Q ARE RESULTANT FORCES

FIGURE 11.—FORCE DIAGRAMS FOR ACTIVE AND PASSIVE EARTH PRESSURES.

case is that of Coulomb and this method deals with forces rather than stresses. One basic assumption is that the surface of failure is, for all practical purposes, a plane (actually it is more nearly an arc of a circle having a large radius of curvature). The solution is then briefly as follows:

In figure 11, let θ be the angle between the plane of failure and the horizontal, and W the weight of earth which slides when the earth fails. It is assumed that the magnitude of θ is such that the resultant force, E , against the wall is a maximum or, that if E is some function of θ , then $\frac{dE}{d\theta} = 0$. It is further assumed that ϕ' , the angle of friction between the wall and the earth, is less than ϕ , the angle of internal friction of the earth.

Assume for the present (see fig. 11) that the positions of the failure planes and the angles ϕ and ϕ' are known. In the upper diagram of figure 11 for active earth pressure the earth moves downward over the sliding plane, whereas in the lower diagram for passive earth pressure movement of earth is upward over the sliding plane. The tangential forces, both along the wall and sliding plane, are therefore opposite in direction in the two cases. Hence the resultant force E against the wall acts below the normal to the wall in the upper diagram and above the normal to the wall in the lower diagram and likewise the relative positions of the resultant force Q and the normal force N on the plane of failure are different in the two cases.

⁸ The Mechanics of Shear Failures on Clay Slopes and the Creep of Retaining Walls, by Charles Terzaghi, PUBLIC ROADS, vol. 10, No. 10, December 1929.

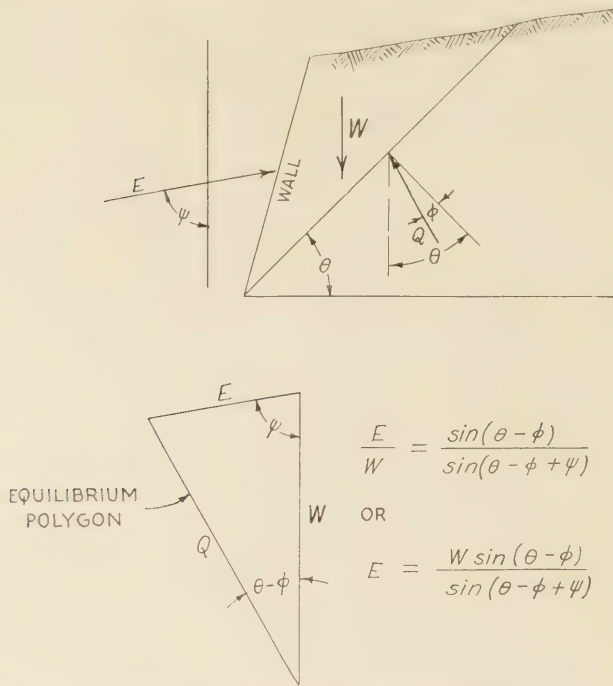


FIGURE 12.—FORCE DIAGRAM AND EQUILIBRIUM POLYGON FOR ACTIVE EARTH PRESSURE.

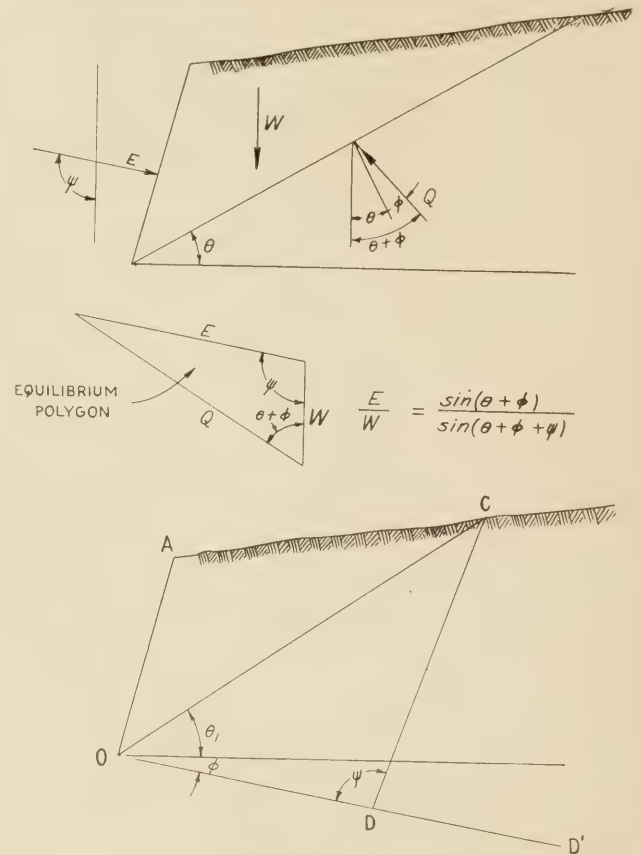


FIGURE 14.—DIAGRAM SHOWING METHOD OF LOCATING THE SLIDING PLANE FOR PASSIVE EARTH PRESSURE.

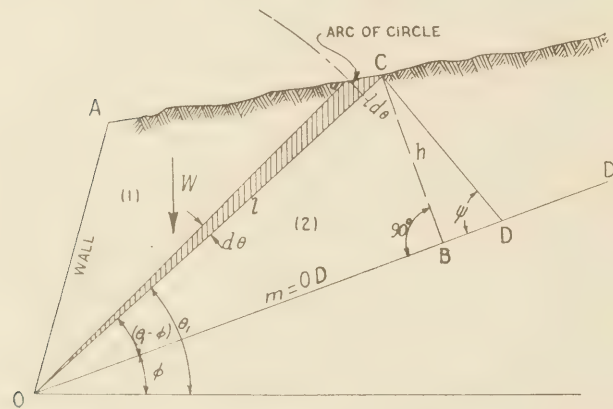


FIGURE 13.—DIAGRAM SHOWING METHOD OF LOCATING THE SLIDING PLANE FOR ACTIVE EARTH PRESSURE.

The position of the plane of failure cannot, however, be assumed. It must be found. For active earth pressure, let ψ be the angle between the direction of E and the vertical (see fig. 12). From the equilibrium polygon of forces, as shown in this figure,

$$E = \frac{W \sin(\theta - \phi)}{\sin(\theta - \phi + \psi)} \quad (23)$$

and, for E to be a maximum,

$$\frac{dE}{d\theta} = 0 = \frac{\sin(\theta - \phi + \psi) \left[\frac{dW}{d\theta} \sin(\theta - \phi) + W \cos(\theta - \phi) \right] - W \sin(\theta - \phi) \cos(\theta - \phi + \psi)}{\sin^2(\theta - \phi + \psi)}$$

That is,

$$W [\sin(\theta - \phi + \psi) \cos(\theta - \phi) - \sin(\theta - \phi) \cos(\theta - \phi + \psi)] = - \left[\frac{dW}{d\theta} \right] \sin(\theta - \phi) \sin(\theta - \phi + \psi)$$

Therefore

$$W = \left[- \frac{dW}{d\theta} \right]_{\theta_1} \frac{\sin(\theta_1 - \phi) \sin(\theta - \phi + \psi)}{\sin \psi} \quad (24)$$

where θ_1 is the value of θ for which E is a maximum.

In figure 13 the line $OC = l$ and the area of the shaded triangle is approximately $\frac{1}{2} l^2 d\theta$. The weight of earth in the shaded triangle is

$$-(dW)_{\theta_1} = \frac{1}{2} w l^2 (d\theta)_{\theta_1}$$

or

$$\left[- \frac{dW}{d\theta} \right]_{\theta_1} = \frac{1}{2} w l^2 \quad (25)$$

Draw OD' , inclined at the angle ϕ with the horizontal, and draw CD to intersect OD' at the angle ψ . Drop the perpendicular, h , from C to OD' . Then

$$\frac{m}{l} = \frac{\sin[\pi - (\theta_1 - \phi + \psi)]}{\sin \psi} = \frac{\sin(\theta_1 - \phi + \psi)}{\sin \psi}$$

where $m = OD$. Furthermore, $\frac{\sin(\theta_1 - \phi)}{\sin 90^\circ} = \frac{h}{l}$ and substituting this value, together with $\frac{m}{l}$ and $\frac{1}{2} w l^2$ from formula (25) in formula (24), there is obtained

$$W = \frac{1}{2} w l^2 \times \frac{h}{l} \times \frac{m}{l} = \frac{whm}{2} \quad (26)$$

Hence W is equal to the area $COD \times w$ (fig. 13). Obviously for a maximum active earth pressure, the area $OACD$ (fig. 13) must be divided equally so that the area of the triangle AOC = area of COD , and CD may be moved parallel to itself until this condition obtains, and triangle (1) is equal in area to triangle (2) (fig. 13).

For determining passive pressures, except for minor changes, the procedure is the same as that for active pressures. The slight differences are shown in figure 14. Here the line OD' is drawn below the horizontal rather than above it, the angle between OD' and the horizontal being ϕ in both active and passive pressure diagrams. For passive earth pressure (see fig. 14),

$$E = \frac{W \sin(\theta + \phi)}{\sin(\theta + \phi + \psi)} \quad (27)$$

Setting $\frac{dE}{d\theta} = 0$ as before and designating the value of θ

for which E is a maximum as θ_1 ,

$$W = \left[-\frac{dW}{d\theta} \right]_{\theta_1} \frac{\sin(\theta_1 + \phi) \sin(\theta_1 + \phi + \psi)}{\sin \psi} \quad (28)$$

and except for the sign of ϕ , formula (28) is the same as (24), which is for active earth pressure. By moving the line CD (which makes an angle, ψ , with OD'), parallel to itself, its position when the area of triangle OAC = area OCD , meets the requirement that E is a maximum and therefore that OC is the sliding plane.

MAXIMUM EARTH STRESSES MUST BE PROVIDED FOR IN DESIGN

There are various graphical procedures⁹ used in computing active and passive earth pressures and their distributions against retaining walls. The procedures are merely simplified forms of the foregoing combined analytical and graphical procedures. In addition to simplification, it is on the side of safety to take ϕ' as zero. The pressure distribution against the wall is triangular, increasing from zero at the top to a maximum at the base. The resultant force (total pressure), E , is considered as applied at the intersection of the medians of this triangle, and this is one-third of the distance upward from the base of the fill.

Vertical pressure under an abutment.—Because of an overturning moment¹⁰ caused by any of the three earth pressures (active, passive, or earth pressure at rest) the vertical pressure distribution under an abutment is in general trapezoidal (see fig. 5), the greatest pressure, p_0 , being directly under the toe. As shown previously in this paper, if the cohesion of the supporting soil exceeds $\frac{p_0}{\pi}$ there is no danger of failure of the undersoil.

On the other hand, if the cohesion is less than $\frac{p_0}{\pi}$, failure of the undersoil is not inevitable.

One may go farther in this case and apply the general method of Hogentogler and Terzaghi¹¹ in investigating the stability of the supporting soil. The analysis is illustrated in figure 15. In computing the greatest shearing stress at any point in the undersoil and also in

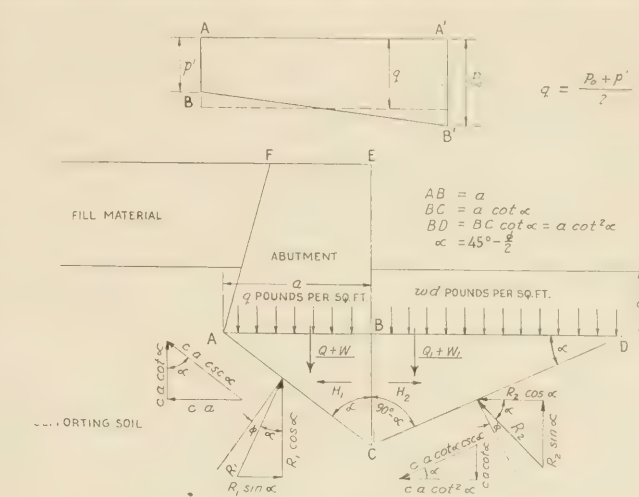


FIGURE 15.—DIAGRAM SHOWING METHOD OF COMPUTING SUPPORTING POWER OF SOIL BELOW BRIDGE ABUTMENT.

connection with any computations of settlement of the abutment (fig. 15) resulting from slow consolidation of one or more compressible soil strata below the abutment, it is necessary to determine the load diagram (such as $AA'B'B$, upper diagram of fig. 15) and use it without transformation. However, in the following investigation of the possibility of the development of surface failure in the supporting soil (ACD , fig. 15) it is on the side of safety to consider the load transmitted by the wall or abutment as uniformly distributed along the plane, AB . For since the wedge, ABC , tends to move downward along the plane, AC , and push out and upward the wedge, BCD , along the plane, CD , it is obvious that an excess of pressure at B over that at A offers resistance to the forward movement of the wedge, ABC .

FORCES COMPUTED FOR CONDITIONS OF EQUILIBRIUM

With reference to figure 15, the average pressure along AB is $\frac{p' + p_0}{2} = q$, and it is assumed that this acts uniformly over AB . The vertical section is supposed to be of unit thickness in the direction perpendicular to the plane of the paper. Neglecting frictional resistance along AB and the shearing resistance of the surcharge of thickness, d , above the plane, BD , is again on the side of safety and simplifies the problem. Use is now made of the principles of active and passive earth pressures. The angle $\alpha = 45^\circ - \frac{\phi}{2}$. The shearing plane for active earth pressure, as already shown, is inclined at an angle of $45^\circ - \frac{\phi}{2}$ with the vertical, and the shearing plane for passive earth pressure is inclined at $45^\circ + \frac{\phi}{2} = 90^\circ - \alpha$ to the vertical (see figs. 8 and 9). Assume that the unit weight, w , of the undersoil is constant throughout the region indicated in figure 15. Computations will be made in terms of forces and not stresses.

The total vertical load on AB , of width a , is equal to $Q = qa$. The weight of the wedge, ABC , is $\frac{w(AB \times BC)}{2}$ or weight = $\frac{wa^2 \cot \alpha}{2} = W$. Then the total vertical force acting on the wedge, ABC , is $aq + \frac{wa^2 \cot \alpha}{2}$

⁹ See for example, Notes on Soil Mechanics and Foundations, by Fred L. Plummer (Edwards Brothers, Inc., Ann Arbor, Mich.), pp. 123 to 130, inclusive. See also pl. No. 17, p. 20, booklet, Soil Stabilization, published by the American Road Builders' Ass'n, 1938.

¹⁰ For methods of computing the overturning and resisting moments, see pl. No. 16 p. 19, booklet, Soil Stabilization, published by the American Road Builders' Ass'n., 1938.

¹¹ Interrelationship of Load, Road and Subgrade, by C. A. Hogentogler and Charles Terzaghi, Public Roads, vol. 10, No. 3, May 1929.

This downward force is resisted by the vertical component of the cohesion along AC , which is $ca \cot \alpha$ and by the vertical component, $R_1 \cos \alpha$, where R_1 is the resultant of the normal and frictional forces on AC . Then for a condition of equilibrium,

$$R_1 \cos \alpha + ca \cot \alpha = aq + \frac{wa^2 \cot \alpha}{2}$$

or

$$R_1 \cos \alpha = aq + \frac{wa^2 \cot \alpha}{2} - ca \cot \alpha \quad (29)$$

Similarly for equilibrium $R_1 \sin \alpha - ca = H_1$ or

$$R_1 \sin \alpha = H_1 + ca \quad (30)$$

Dividing equation (30) by (29),

$$\tan \alpha = \frac{H_1 + ca}{aq + \frac{wa^2 \cot \alpha}{2} - ca \cot \alpha}$$

Hence

$$H_1 = \frac{wa^2}{2} + aq \tan \alpha - 2ca \quad (31)$$

Now consider forces acting on the wedge, BCD . The weight of the surcharge on the plane, BD , is $wd \times BD$ or $wd a \cot^2 \alpha = Q_1$. The weight of the wedge, BCD , is $\frac{w}{2} BC \times BD = \frac{1}{2} wa^2 \cot^3 \alpha = W_1$. The total downward force is then $Q_1 + W_1$ and this together with the vertical component of the cohesive resistance along CD must equal the upward component, $R_2 \sin \alpha$ for a condition of equilibrium to obtain. That is,

$$R_2 \sin \alpha = \frac{wa^2 \cot^3 \alpha}{2} + wda \cot^2 \alpha + ca \cot \alpha \quad (32)$$

Similarly,

$$R_2 \cos \alpha = H_2 - ca \cot^2 \alpha \quad (33)$$

Dividing equation (32) by (33) and solving for H_2 ,

$$H_2 = \frac{wa^2 \cot^4 \alpha}{2} + wda \cot^3 \alpha + 2ca \cot^2 \alpha \quad (34)$$

For equilibrium, $H_1 = H_2$ and from equations (31) and (34), therefore,

$$\frac{wa^2}{2} + aq \tan \alpha - 2ca = \frac{wa^2 \cot^4 \alpha}{2} + wda \cot^3 \alpha + 2ca \cot^2 \alpha$$

and hence

$$q = \frac{2c}{\tan \alpha \sin^2 \alpha} + \frac{wa}{2 \tan \alpha} \left[\frac{1}{\tan^4 \alpha} - 1 \right] + \frac{wd}{\tan^4 \alpha} \quad (35)$$

where q is the bearing capacity or supporting power of the undersoil. For $\phi = 0$, as is the case in a purely cohesive soil, $q = 4c + wd$, which means that the supporting power is independent of a , the width of the bearing area. In a compression test of an unconfined cylinder of the purely cohesive soil, $p_h = 0$ and $p_v =$ compressive strength $= 2c$, since $c = \frac{p_v - p_h}{2} = \frac{p_v}{2}$. Hence for such a soil and with reference to figure 15, the supporting power, q , is equal to twice the compressive strength

(as determined in an unconfined cylinder compression test) plus wd .

If the supporting soil is clay, ϕ is small and

$$q = 4c + wd \quad (36)$$

is a safe working formula. Therefore if the supporting undersoil is clay, the design engineer is first of all concerned with the relative magnitudes of the cohesion and $\frac{p_0}{\pi}$. If the cohesion is greater than $\frac{p_0}{\pi}$ (the cohesion being a conservative value based on the allowable displacement of the structure), the problem ends there.

If the cohesion is less than $\frac{p_0}{\pi}$, then q must not exceed $4c + wd$ in any case, the value q being the average unit vertical load transmitted by the wall or abutment to the undersoil. For conditions in which ϕ is greater than zero, q may be computed directly from equation (35).

METHOD BASED ON PLANE STRAIN HAS LIMITATIONS

For a uniform surface load over a long strip of parallel sides, Prandtl's method¹² yields $q = 5.14c$ for a purely cohesive soil, $\phi = 0$, and for the same conditions the method of Krey¹³ gives $q = 6.6c$.

The legitimate use of the formulas for plane strain in connection with abutment and retaining wall problems depends chiefly on the ratio of length to width of the footing. There have apparently been no rules as to procedures where this ratio is small. Furthermore, for a rectangular footing whose length is not great in comparison to its width, there are apparently no formulas for stresses other than the vertical one, p_z and the lateral ones p_x and p_y , to be found in current literature. It is interesting therefore to compute p_z for a relatively long footing both by the formula as applicable to the case of plane strain and by the formula for the case involving three dimensions. It should be noted that p_z is independent of elastic constants in either method of computation, and it is the only stress having this characteristic.

In order to indicate the limitations of the method based on plane strain, four different footings will be considered. These are:

No. 1.....	50 feet long, 8 feet wide.
No. 2.....	35 feet long, 10 feet wide.
No. 3.....	30 feet long, 10 feet wide.
No. 4.....	20 feet long, 10 feet wide.

It is assumed that there is a uniform load distribution of 3 tons per square foot on each of these four footings. The vertical pressure, p_z , at any point in the earth at a depth of z feet below the footing is then computed by two different methods. These are:

- The method based on plane strain.
- The method based on rectangles using Newmark's tables¹⁴ for convenience.

Newmark's method is both convenient and precise. Another method has been shown in a previous publication¹⁵ and in its use the rectangular footing is sub-

¹² Über die Harte Plastischer Körper Nachrichten von der Gesellschaft der Wissenschaften zu Göttingen, Mathematisch Physikalische Klasse, pp. 74-85, 1920.

¹³ Erddruck Erdwiderstand und Tragfähigkeit des Baugrundes, H. Krey, pp. 193 and 268.

¹⁴ Simplified Computation of Vertical Pressures in Elastic Foundations, by Nathan M. Newmark, Circular No. 24, vol. 33, No. 4, Engineering Experiment Station, University of Illinois, Sept. 24, 1935.

¹⁵ The Theory of Soil Consolidation and Testing of Foundation Soils, by L. A. Palmer and E. S. Barber, PUBLIC ROADS, vol. 18, No. 1, March 1937.

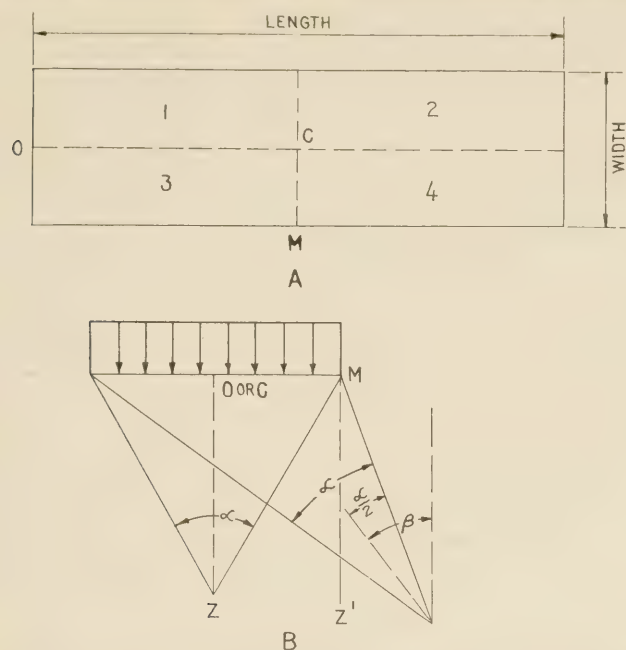


FIGURE 16.—DIAGRAM SHOWING VALUES INVOLVED IN COMPUTING THE NORMAL STRESS p_z .

divided into elements. The load on each element of area is then considered as a point load at the center of the element of area. The computation of p_z by either method, (a) or (b), involves no elastic constants. The formulas for p_z as developed by Boussinesq for a point load and as extended by others do not involve elastic constants.

With reference to figure 16A, p_z will be computed for depths of 5, 10, 15, and 20 feet along vertical lines through the points, C , the center of footing, O , the midpoint of an end, and M , the midpoint of a side. For the method of plane strain, the general formula is

$$p_z = \frac{p}{\pi} (\alpha + \sin \alpha \cos 2\beta) \dots \dots \dots (37)$$

where α and β are the angles shown in figure 16B. Along the vertical line CZ , $2\beta = 0$ and formula (37) becomes

$$p_z = \frac{p}{\pi} (\alpha + \sin \alpha) \dots \dots \dots (38)$$

Along the vertical line, OZ , for points below O at the end of the footing, half the value of p_z as determined by formula (38) must be taken. For points on MZ' figure 16B, $2\beta = \alpha$.

Newmark's tables are based on values for p_z at points on a vertical line through a corner of rectangles of various sizes. Thus, the point, C , of figure 16A is a corner common to each of the four rectangles, 1, 2, 3, and 4, all of the same dimensions. The value p_z for a point on CZ is first obtained for one of these rectangles, and this value multiplied by 4 gives p_z (for a point on CZ) as resulting from the load on the entire footing. Similarly, the point, O is a corner, common to the two rectangles, 1 and 2, taken together and 3 and 4 taken together.

An example will clarify the two methods of computing p_z . It is desired to know p_z at 20 feet below the point, C , for footing No. 3, 10 feet by 30 feet, the unit load being 3 tons per square foot. The rectangles, 1, 2, 3, and 4 are each 5 feet by 15 feet,

$$\sin \alpha = 2 \sin \frac{\alpha}{2} \cos \frac{\alpha}{2} = 2 \left[\frac{5}{\sqrt{425}} \times \frac{20}{\sqrt{425}} \right] = \frac{200}{425} = 0.471$$

and hence $\alpha = 0.490$ in radians. Then by formula (38),

$$p_z = \frac{3}{\pi} (0.490 + 0.471) = 0.92 \text{ tons per square foot.}$$

From Newmark's tables, $m = \frac{5}{20} = 0.25 =$ the width of one of the rectangles, 1, 2, 3, or 4, divided by the depth,

$$20 \text{ feet, and } n = \frac{\text{length}}{\text{depth}} = \frac{15}{20} = 0.75. \text{ The "coefficient"}$$

corresponding to $m = 0.25$ and $n = 0.75$ is 0.05986. This is first multiplied by 4 for the 4 rectangles and then by 3 tons per square foot, that is,

$$p_z = 0.05986 \times 12 = 0.72 \text{ tons per square foot.}$$

In this manner, the values for p_z in table 1 are computed for the footings, 8 by 50 feet, 10 by 35 feet, 10 by 30 feet, and 10 by 20 feet, each with a uniform load of 3 tons per square foot, and at various depths below the points C , O , and M (fig. 16).

TABLE 1.—Values of p_z computed by methods based on plane strain and on rectangles, assuming a uniform loading of 3 tons per square foot

Size of footing (feet)	Depth of point considered	Vertical pressure, p_z					
		Below point C by method based on—		Below point O by method based on—		Below point M by method based on—	
		Plane strain	Rectangles	Plane strain	Rectangles	Plane strain	Rectangles
10 by 20	Feet 5	2.46	2.40	1.23	1.23	1.44	1.39
	10	1.65	1.44	.82	.81	1.23	1.05
	15	1.28	.94	.64	.57	1.02	.75
	20	.92	.57	.46	.40	.82	.50
10 by 30	5	2.46	2.44	1.23	1.23	1.44	1.43
	10	1.65	1.57	.82	.82	1.23	1.16
	15	1.28	1.02	.64	.60	1.02	.90
	20	.92	.72	.46	.44	.82	.64
10 by 35	5	2.46	2.45	1.23	1.23	1.44	1.43
	10	1.65	1.60	.82	.82	1.23	1.18
	15	1.28	1.12	.64	.60	1.02	.94
	20	.92	.77	.46	.44	.82	.69
8 by 50	5	2.22	2.22	1.11	1.11	1.40	1.39
	10	1.39	1.37	.69	.69	1.11	1.10
	15	.92	.88	.46	.46	.82	.82
	20	.74	.69	.37	.37	.69	.64

RESULTS OBTAINED BY TWO METHODS COMPARED

For a given footing it is seen in table 1 that the difference in values for p_z as computed by the two methods increases with depth. The method based on plane strain is based on the assumption that the loaded foundation is of "infinite" length. Only finite lengths are considered in table 1 and for this reason the values obtained by the method based on rectangles are considered to be the correct ones.

In the light of present knowledge it is not possible to compute shearing stresses by the method based on rectangles but it is possible to do this by the method based on plane strain. As indicated previously it is necessary to know the shearing stresses and for this reason it is desirable to use the method based on plane strain when the error involved in so doing is not too large. Since it is possible to compute p_z for different points at a given depth by both methods, it should be reasonable to assume that if the values so computed are in fairly good agreement, then the analytical

method illustrated in figure 15 and based on the assumption of plane strain conditions is applicable in any case when the failure plane (*AC*, fig. 15) does not extend below the depth in question.

In making use of table 1 it should be borne in mind that the ratio of width to length of a footing is the important consideration. Thus, any conclusion reached with respect to the footing that is 10 feet wide and 30 feet long is applicable also to a footing that is 20 feet wide and 60 feet long, or 5 feet wide and 15 feet long, etc.

Another point to be considered is the following: In figure 15, illustrating failure under an abutment, the soil moves out in but one direction, that is, along plane *CD* which is on the open side of the abutment or retaining wall. The depth *BC* in this case is the width, *a*, multiplied by $\cot\left(45^\circ - \frac{\phi}{2}\right)$. Thus, for $\phi=0$, *BC* (the depth to which the failure plane *AC* extends) is equal to *a*. On the other hand the supporting soil under a bridge pier is free to move out in two directions rather than but one. Then from symmetry the depth to which the failure plane extends under a pier is $\frac{a}{2} \cot\left(45^\circ - \frac{\phi}{2}\right)$ where *a* is the width of the pier.

To illustrate, if the 10 by 30-foot footing of table 1 is a bridge pier and if $\phi=0$, the plane of failure extends to a depth of 5 feet below the pier. For points at this depth it is seen in table 1 that the values for p_z computed by the two methods is in good agreement. On the other hand if the base of an abutment has these same dimensions and ϕ of the supporting soil is zero, then the failure plane extends downward to a depth=*a*=10 feet and for this depth there is greater divergence in the two sets of computed values of p_z . The more serious consideration then is that of the abutment or retaining wall where the failure plane extends to twice the depth that obtains in the case of a pier.

As ϕ increases, $\cot\left(45^\circ - \frac{\phi}{2}\right)$ increases and the depth (*BC* figure 15)=*a* × $\cot\left(45^\circ - \frac{\phi}{2}\right)$ increases. A few computed values are as follows:

ϕ , degrees	Depth of failure plane
0	<i>a</i>
10	1.19 <i>a</i>
20	1.43 <i>a</i>
22	1.48 <i>a</i>
30	1.73 <i>a</i>
38	2.05 <i>a</i>

For $\phi=0$ and for a bridge pier of the dimensions shown in table 1, the failure plane extends down to 4 feet below the last footing and to 5 feet below the other three. Since at this depth the agreement in the two sets of computed p_z values is good in all cases, it is concluded that for any bridge pier having the same relative dimensions as those shown in table 1, the analytical method, assuming the method based on plane strain, is well warranted if $\phi=0$. If the first footing is excepted the same conclusion is reached in the case of abutments or retaining walls of the same relative dimensions. In this case the plane of failure extends down to 10 feet below the first three footings. The divergence in p_z , 1.57 to 1.65 tons per square foot below point *C* and 1.16 to 1.23 below point *M* (fig. 16) at 10 feet below the 10×30-foot footing is not considered as being serious.

By the same reasoning it is concluded that if the failure plane does not extend below 1½ times the width of the base of the abutment or retaining wall, the analytical method assuming plane strain conditions is warranted for any footing having a length-to-width ratio of 3 or greater. This includes all types of supporting soils having a value of ϕ of about 22°. The value of ϕ for most clays seldom exceeds 20° and this type of soil is usually the most dangerous insofar as supporting power is concerned. Values of ϕ exceeding 20° are characteristic of soils of considerable sand content. The value of ϕ for sands ranges usually from 35 to 40°, an approximate average value being 38° for which the failure plane extends to a depth of 1.73*a* for an abutment and to 0.87*a* for a pier.

CONCLUSIONS

The following conclusions are believed warranted:

1. The analytical method, assuming plane strain conditions, is applicable for all bridge piers of the relative dimensions given in table 1 (length-to-width ratio of 2 or greater) and for all values of ϕ ranging from 0 to values characteristic of sand.
2. The same analytical method is warranted for bridge abutments and retaining walls when the length-to-width ratio of the base is 3 or greater, ϕ having any value ranging from 0 to 22°. This includes practically all clays which present the major problem with respect to supporting power.

In the absence of percolating water or hydrostatic uplift, sands do not generally present a serious problem.

It is possible to check the accuracy of the assumption of conditions of plane strain by computations of the stress, p_z . It is not possible to check the assumption by computations of values of all other stresses. On account of this fact there is no check on the reasonableness of the assumption of conditions of plane strain other than the agreement of p_z values as computed by the method based on rectangles and by the method based on plane strain. A study of past and current soil mechanics literature does not indicate any means of computing by methods using three dimensions the shearing stresses at points below a rectangular loaded area.

The problem has, however, been solved in part for a loaded circular area¹⁶ and Jürgenson¹⁷ computes the stresses below a square footing by assuming a circle of equivalent area. For the loaded circular area, the analysis is limited to merely computing the stresses at any point below. Thus, it is known that the greatest

shearing stress is equal to $\frac{p}{\pi}$, where *p* is the unit load (when the load distribution is uniform) and this shearing stress exists at all points immediately beneath the perimeter.

For a circular footing there is as yet no solution to the problem of determining the supporting power of the undersoil when *c*, the unit cohesion, is less than $\frac{p}{\pi}$.

Nadai¹⁸ shows that on the basis of experiment the forcing of a punch of cylindrical cross section into a plastic metal produces flow figures in the shape of logarithmic spirals, and the same phenomenon is ob-

¹⁶ Treatise on the Mathematical Theory of Elasticity (see p. 190), by A. E. H. Love, 4th ed. Cambridge, University Press, 1934.

¹⁷ The Application of Theories of Elasticity and Plasticity to Foundation Problems, by Leo Jürgenson, Journal of the Boston Society of Civil Engineers, vol. 21, No. 3, July 1934.

¹⁸ Plasticity, A. Nadai, p. 228, McGraw-Hill Book Co., 1931.

served in the heads of boilers subjected to plastic bending under an axially symmetrical stress field. There is, however, no adequate theory to account for this occurrence.

Only rigid footings and static loads have been assumed and considered in this paper. The case of flexible footings presents complicated factors which for the most part have not as yet been satisfactorily accounted for. The problem of dynamic loading still awaits a theoretical solution substantiated by ample experimental data.

THE COVER PICTURE

The value of preserving trees and protecting them from damage during highway construction is shown by the cover picture. This section of U. S. Highway No. 1, near Brunswick, Maine, passes through a pine forest known as "The Bowdoin Pines."

Modern highways are designed so as to preserve the natural beauty of the roadside without sacrifice of service or utility. This has been successfully done on the highway shown. Here the grade of the highway is at approximately the same elevation as the surface of the adjacent ground. Note how the undergrowth screens the bases of many of the large trees, and how inconspicuous the poles and wires become.

STATUS OF FEDERAL-AID HIGHWAY PROJECTS

AS OF NOVEMBER 30, 1938

STATE	COMPLETED DURING CURRENT FISCAL YEAR			UNDER CONSTRUCTION			APPROVED FOR CONSTRUCTION			BALANCE OF AVAILABLE FEDERAL-GRANTED PROJECTS
	Estimated Total Cost	Federal Aid	Miles	Estimated Total Cost	Federal Aid	Miles	Estimated Total Cost	Federal Aid	Miles	
Alabama	\$ 2,882,571	\$ 1,747,485	82.8	\$ 8,249,172	\$ 4,113,175	354.9	\$ 2,376,954	\$ 1,187,935	67.2	\$ 2,102,846
Arizona	1,906,924	1,483,382	107.5	889,645	574,320	24.9	333,503	140,345	25.8	1,106,569
Arkansas	938,120	933,384	70.0	3,032,208	3,028,471	184.9	542,108	542,003	39.1	723,592
California	6,503,704	3,533,424	132.4	7,793,061	4,153,140	141.9	1,671,940	884,689	45.3	1,279,156
Colorado	1,974,682	1,065,932	73.2	3,304,793	1,744,317	102.0	810,660	450,740	21.8	1,470,339
Connecticut	183,510	89,250	2.4	1,190,108	583,050	12.3	244,930	120,990	2.0	1,525,005
Delaware	446,780	281,184	13.6	711,750	333,895	9.9	265,351	128,530	6.6	1,137,482
Florida	1,184,100	582,050	36.9	3,589,938	1,794,969	60.0	277,000	138,500	3.9	2,841,192
Georgia	3,762,708	1,839,849	195.1	5,444,474	2,722,237	253.8	404,770	404,770	57.1	5,365,212
Idaho	2,024,215	1,199,579	194.5	11,101,321	657,611	33.6	99,697	59,667	5.4	1,097,803
Illinois	4,872,534	2,432,095	156.6	11,106,011	5,551,699	239.6	1,242,791	621,350	35.7	2,214,901
Indiana	4,213,808	2,101,210	117.5	3,836,480	821,699	76.5	1,659,490	81,599	32.2	2,191,813
Iowa	6,271,239	2,922,519	205.2	5,284,744	2,350,883	178.3	718,778	336,500	24.2	83,747
Kansas	4,074,179	2,017,365	68.7	4,294,889	2,122,392	217.0	3,397,658	1,637,819	164.3	2,455,720
Kentucky	5,042,152	2,505,062	183.5	3,225,314	1,612,657	75.1	914,208	457,104	25.5	2,190,356
Louisiana	1,049,009	584,310	36.1	11,507,992	2,148,774	32.5	1,761,038	775,592	28.6	2,272,042
Maine	2,606,505	1,298,831	61.9	1,476,101	738,050	32.6	227,424	113,711	1.9	160,661
Maryland	520,000	260,000	8.6	2,333,767	1,150,121	40.9	1,034,781	498,730	13.1	1,670,916
Massachusetts	1,581,901	790,948	7.1	2,862,339	1,431,167	16.4	771,127	383,820	11.4	2,200,384
Michigan	6,355,735	3,081,704	132.5	4,664,328	2,330,647	134.8	942,775	453,170	14.8	1,350,304
Minnesota	3,605,384	1,743,673	200.2	6,566,335	3,280,535	317.8	1,153,760	575,975	61.2	1,888,013
Mississippi	1,654,408	785,862	63.5	9,285,812	3,531,207	409.5	2,387,560	974,250	92.2	1,734,726
Missouri	3,932,508	1,890,869	113.9	2,595,248	1,287,136	59.2	5,011,716	2,272,236	194.0	2,753,696
Montana	1,666,619	936,796	83.6	703,682	395,460	16.4	312,764	165,665	9.6	4,315,758
Nebraska	2,993,074	1,496,429	299.7	5,525,012	2,724,035	415.7	4,056,160	1,394,528	263.6	1,450,619
Nevada	1,002,368	856,482	151.4	1,004,456	864,644	33.6	806,942	699,279	34.8	676,332
New Hampshire	881,761	437,187	21.5	437,424	217,752	3.3	93,802	46,900	1.4	1,141,725
New Jersey	793,715	388,600	6.3	2,786,016	1,390,128	19.8	895,990	447,165	9.6	2,254,697
New Mexico	1,966,562	1,198,902	220.1	1,481,057	1,003,464	68.0	1,022,421	580,234	57.3	295,370
New York	10,831,152	5,342,590	206.8	12,032,857	5,942,662	190.2	2,636,100	1,067,150	45.6	921,204
North Carolina	5,841,282	2,801,559	228.1	5,209,119	2,598,582	336.9	815,080	395,150	45.3	1,660,945
North Dakota	3,322,708	3,191,747	254.8	456,801	287,254	56.9	85,822	44,787	7.4	3,568,606
Ohio	5,627,144	2,787,529	68.7	9,580,762	4,762,200	93.0	1,789,340	891,514	19.2	5,487,881
Oklahoma	4,269,577	2,256,996	182.5	3,931,773	2,039,695	114.8	1,980,100	1,037,467	44.1	2,144,066
Oregon	2,874,047	1,693,690	106.8	1,225,473	740,297	62.6	917,078	559,320	50.1	1,427,148
Pennsylvania	6,439,721	3,198,425	111.5	7,493,866	3,739,756	83.7	3,411,363	1,686,038	34.8	2,319,486
Rhode Island	1,131,980	565,990	16.1	409,982	202,961	3.9	73,900	36,950	0.6	1,028,984
South Carolina	3,470,957	1,524,748	204.8	3,977,180	1,789,376	112.2	480,641	253,700	18.0	1,244,352
South Dakota	1,207,492	985,571	215.0	4,411,146	2,434,470	400.3	772,880	427,270	91.9	2,565,496
Tennessee	2,627,760	1,313,880	95.0	4,319,134	2,159,567	102.2	1,291,960	645,480	28.3	3,872,020
Texas	9,845,961	4,873,446	666.3	9,682,145	4,649,822	441.1	5,851,109	2,845,867	246.8	4,405,759
Utah	1,111,437	785,540	114.7	1,869,040	1,329,150	65.4	182,350	128,000	6.4	575,283
Vermont	1,128,228	548,588	32.3	808,484	379,703	20.3	196,970	98,895	4.3	161,742
Washington	5,218,591	2,607,165	181.5	3,342,173	1,669,251	104.4	697,992	346,891	14.9	571,664
West Virginia	3,897,164	2,052,732	91.8	2,535,423	1,329,759	23.2	331,657	177,400	3.1	677,739
Wisconsin	1,322,093	874,029	43.6	1,637,996	995,455	44.9	850,210	421,255	22.7	1,995,228
Wyoming	3,826,117	1,863,271	126.7	6,888,313	3,259,780	199.2	164,594	78,000	0.2	3,799,283
District of Columbia	2,430,882	1,489,487	286.3	244,882	145,791	20.3	343,570	212,540	51.0	534,495
Puerto Rico	517,508	258,624	9.9	1,132,210	557,165	17.4	17,860	6,630	0.3	1,202,757
TOTALS	154,490,584	80,969,973	6,859.5	198,662,145	97,386,077	6,082.8	59,061,194	28,864,560	2,090.6	90,171,545

STATUS OF FEDERAL-AID GRADE CROSSING PROJECTS

AS OF NOVEMBER 30, 1938

STATE	COMPLETED DURING CURRENT FISCAL YEAR				UNDER CONSTRUCTION				APPROVED FOR CONSTRUCTION				BALANCE OF FUNDS AVAILABLE FOR OTHER PROJECTS	
	Estimated Total Cost	Federal Aid	NUMBER		Estimated Total Cost	Federal Aid	NUMBER		Estimated Total Cost	Federal Aid	NUMBER			
			Grade Eliminated by Separation Rejection	Grade Crossing Struts or other			Grade Eliminated by Separation Rejection	Grade Crossing Struts or other			Grade Eliminated by Separation Rejection	Grade Crossing Struts or other		
Alabama	\$ 252,184	\$ 252,110	6	4	\$ 555,574	\$ 554,624	5	1	\$ 402,505	\$ 401,600	4	3	\$ 777,185	
Arizona	46,565	45,688	3		9,452	9,452	9		177,787	177,678	3		620,761	
Arkansas	669,417	669,417	2	2	497,443	497,052	9	6	719,415	718,935	3	18	1,817,062	
California	30,465	27,859	1		61,728	61,728	1		120,759	116,999	1		1,081,746	
Connecticut					18,530	12,665							831,825	
Delaware	24,500	24,500		7									407,330	
Florida					215,316	215,316	2		207,100	207,100	1		983,381	
Georgia					96,720	96,720	2		305,230	305,230	4		2,015,437	
Ideho	174,973	174,800	4		263,415	249,386	4						398,684	
Illinois	286,500	286,500	2	1	1,618,825	1,618,825	3	2	1,040,690	1,040,690	7	66	2,258,628	
Indiana	408,486	322,500	2	3	1,032,980	1,006,080	3	3	271,000	271,000	1		814,569	
Iowa	951,320	900,897	9	14	265,413	249,900	3	5	47,124	44,200	1	2	1,372,564	
Kansas	456,074	456,074	8	4	605,225	605,225	9	2	532,921	532,921	5	6	980,288	
Kentucky	145,000	145,000	1		291,525	291,525	2	1	494,414	494,414	8	1	883,106	
Louisiana					225,285	196,478	3	2	476,771	473,090	10		907,503	
Maine	48,590	48,590	2		327,315	327,315	3	2	69,830	69,830	1		245,468	
Maryland					64,586	64,586	1						962,247	
Massachusetts	54,710	54,710	1		220,486	220,486	1		222,275	220,344	3		1,417,944	
Michigan	893,783	887,372	8	16	622,336	622,336	6	1	80,690	80,690	1		1,694,787	
Minnesota	40,218	40,218	1	1	760,185	759,864	3	5	18,297	18,297	1	3	1,626,755	
Mississippi					465,800	465,800	6		250,000	250,000	1		868,251	
Missouri	128,514	127,392	2	1	279,530	279,530	3	3	397,960	397,960	1	1	2,220,371	
Montana	355,586	350,704	4	4	449,518	449,518	4	4	409,042	409,042	5		115,207	
Nebraska	150,374	150,374	4		390,393	390,393	10		738,215	738,215	20		485,428	
Nevada	97,187	97,187	1		55,074	55,074	1		231,055	231,055	2		75,325	
New Hampshire	61,732	61,425	1	2	51,547	51,547	5	1	4,590	4,590	2		336,188	
New Jersey	116,891	111,665	1	1	223,914	223,914	1	1					1,634,678	
New Mexico	168,984	168,984	4	1	118,994	118,994	3	2	284,420	189,030	2	1	563,513	
New York	141,400	141,400	1	2	2,447,252	2,438,751	9	8	147,030	147,030	1	11	4,000,748	
North Carolina					917,500	884,800	7	5					1,359,014	
North Dakota	73,550	73,550	1		822,138	822,138	4	2					757,083	
Ohio					95,850	95,850	2		640,700	640,700	7		3,492,618	
Oklahoma	308,391	307,742	1	2	17,343	17,343			250,305	250,305	1	55	2,013,861	
Oregon	138,043	128,837	1		58,654	58,654			129,997	129,997	2		478,958	
Pennsylvania					304,601	299,694	2		1,259,577	1,240,792	3		4,069,212	
Rhode Island					335,019	335,019	1	2	123,785	123,785	1		34,946	
South Carolina	20,930	20,930			164,359	109,393	3	2	335,820	335,820	12	40	1,022,959	
South Dakota	99,540	99,540	1	8	241,918	241,918	2	2	89,610	89,610	4	3	888,632	
Tennessee					14,381	14,381			320,910	320,910	1	2	1,556,742	
Texas	34,033	33,377	2		1,219,829	1,218,452	12	5	425,695	379,260	5		3,712,027	
Utah	97,174	97,174	2	1	47,359	47,359	2		5,319	5,319			423,211	
Vermont	202,882	197,882	6	1	43,274	43,274	1	6	18,330	18,330	1	6	220,966	
Virginia	248,306	248,306	12	1	241,018	241,018	3	1	397,338	397,338	6	1	909,368	
Washington	149,718	147,618	1	2	673,771	673,771	2	2	128,216	128,216	1	9	134,195	
West Carolina	120,100	119,080	1		315,009	315,009	1		175,870	158,870	4	6	731,139	
West Virginia	162,493	162,493	2		1,160,026	1,160,026	12						1,150,920	
Wyoming	158,370	158,370			10,150	10,150			24,840	24,840	1	10	485,370	
District of Columbia					193,200	193,200	3	1	34,262	34,262			291,169	
Hawaii					214,569	214,569	4						300,550	
Puerto Rico													516,330	
TOTALS	7,515,983	7,332,585	92	25	64	20,862,482	178	51	165	12,371,614	11,880,214	128	15	57,665,430

STATUS OF FEDERAL-AID SECONDARY OR FEEDER ROAD PROJECTS

AS OF NOVEMBER 30, 1938

STATE	COMPLETED DURING CURRENT FISCAL YEAR			UNDER CONSTRUCTION			APPROVED FOR CONSTRUCTION			BALANCE OF FUNDS AVAILABLE FOR PRO. GRANTS PROJECTS
	Estimated Total Cost	Federal Aid	Miles	Estimated Total Cost	Federal Aid	Miles	Estimated Total Cost	Federal Aid	Miles	
Alabama	\$ 73,700	\$ 36,850	10.7	\$ 565,005	\$ 281,050	33.3	\$ 262,200	\$ 130,350	5.6	\$ 604,722
Arizona	281,361	187,459	18.6	190,653	116,491	17.5	7,440	5,357	7.4	247,175
Arkansas				84,417	77,799	8.0	267,422	266,718	25.6	519,591
California	672,360	388,635	60.3	1,188,992	641,483	65.3	598,608	324,358	11.9	493,236
Colorado	571,856	306,038	37.3	574,530	299,145	30.1	75,210	39,480	3.0	276,905
Connecticut	48,450	24,205	1.0	62,584	31,132	.5	4,700	2,310		260,631
Delaware				49,590	24,795	10.9	69,994	34,512	11.9	187,568
Florida				112,922	56,461	.6	290,182	145,050	5.3	473,341
Georgia	286,099	109,101	29.4	558,626	279,313	66.5	239,540	112,770	36.0	750,538
Idaho	412,249	180,843	44.6	104,258	51,017	12.7	128,534	76,572	2.6	165,939
Illinois	985,586	492,025	83.2	1,812,092	852,046	117.2	457,700	220,350	35.0	463,730
Indiana	370,100	144,250	42.9	882,500	420,450	83.8	733,248	354,302	62.9	323,436
Iowa	53,690	26,845	8.6	180,426	90,212	7.7	141,936	70,968	40.1	1,298,449
Kentucky	656,862	196,489	62.4	830,684	230,171	46.8	704,551	205,148	68.1	1,130,946
Louisiana				385,320	175,495	34.5	753,262	321,350	59.5	227,291
Maine				285,826	127,796	13.0	187,000	9,350	1.2	15,027
Maryland				45,164	15,787	5.8	308,800	110,355	18.4	286,334
Massachusetts				64,760	32,380	1.4	292,333	145,470	5.8	468,550
Michigan	129,761	63,381	17.2	678,004	339,002	51.0	546,350	273,175	24.0	859,981
Minnesota	217,978	101,203	30.8	484,284	237,735	50.0	421,664	210,832	24.0	829,810
Mississippi				299,000	149,500	23.8	90,000	45,000	8.4	694,427
Missouri				187,360	93,290	15.7	612,860	288,465	109.8	551,584
Montana	271,479	132,333	35.2	13,983	7,865					1,027,170
Nebraska	410,992	204,652	72.2	360,650	187,845	59.9	484,188	234,873	83.7	370,446
Nevada	420,564	361,693	68.8	74,601	61,643	10.2	43,720	26,016	4.8	45,000
New Hampshire	201,355	99,875	4.5	47,226	23,583	1.5	81,281	39,806	2.4	83,611
New Jersey	71,490	35,745	1.8	202,630	99,470	3.2	48,780	17,500	.1	560,058
New Mexico	516,802	315,195	30.7	436,367	207,627	18.3	337,887	192,174	28.8	91,776
New York	1,990,034	991,719	145.6	2,041,800	1,020,900	108.9	178,400	89,200	11.4	260,675
North Carolina	461,268	230,634	48.3	902,084	451,020	80.4	177,160	75,890	14.3	324,311
North Dakota	33,660	18,135	5.5	119,670	64,092	29.3	115,886	62,066	8.5	682,960
Ohio	156,560	78,280	3.8	27,840	13,920		249,800	174,060	19.2	1,565,391
Oklahoma	21,800	11,598	1.1	426,228	225,671	37.2	529,440	298,520	30.9	889,126
Oregon	453,626	266,110	58.5	38,310	23,422	2.1	21,144	12,900	2.9	452,701
Pennsylvania	1,335,720	644,619	99.7	1,605,145	780,641	85.5	824,754	408,877	49.3	282,547
Rhode Island	66,840	33,420	3.5	162,675	81,314	4.8	74,070	37,035	.9	36,122
South Dakota	274,831	123,372	31.0	11,300	6,250		251,400	94,300	21.3	97,239
Tennessee	78,900	39,450	2.3	661,226	257,713	35.8	195,460	91,260	7.2	671,067
Texas	1,561,835	730,571	247.3	1,958,249	853,904	204.1	866,757	392,535	98.4	1,147,759
Utah	403,316	222,870	40.1	222,529	118,625	15.2	53,420	22,360	8.1	186,515
Vermont				90,306	45,153	4.0	43,300	20,500	.5	35,793
Virginia	240,650	108,150	13.8	867,320	383,720	60.4	26,300	13,150	1.9	317,407
Washington	428,077	178,108	43.8	334,946	176,178	26.6	411,332	216,400	29.2	114,030
West Virginia	124,500	62,150	9.5	228,700	114,350	18.1	40,090	20,514	2.7	373,174
Wisconsin	261,201	120,812	6.1	903,452	440,030	47.0	80,514	40,090	2.7	611,296
Wyoming	431,531	266,644	59.0	301,302	186,179	11.9	136,438	84,301	10.4	48,069
District of Columbia				56,250	28,125	2.4	96,700	47,210	4.9	218,750
Puerto Rico	39,770	19,885	1.4	232,480	115,765	13.8	12,454,765	6,050,254	1,000.9	64,015
TOTALS	15,650,290	7,953,692	1,568.2	22,828,665	10,961,324	1,670.3	12,454,765	6,050,254	1,000.9	22,509,642

